Inorganic Chemistry

Article

pubs.acs.org/IC

Octahedral Gyroscope-like Molecules Consisting of Rhenium Rotators within Cage-like Dibridgehead Diphosphine Stators: Syntheses, Substitution Reactions, Structures, and Dynamic Properties

Gisela D. Hess,[†] Tobias Fiedler,[‡] Frank Hampel,[†] and John A. Gladysz*[,‡]

[†]Institut für Organische Chemie and Interdisciplinary Center for Molecular Materials, Friedrich-Alexander-Universität Erlangen-Nürnberg, Henkestraße 42, 91054 Erlangen, Germany

[‡]Department of Chemistry, Texas A&M University, PO Box 30012, College Station, Texas 77842-3012, United States

Supporting Information

ABSTRACT: Reactions of $Re(CO)_5(X)$ (X = Cl, Br) or $[Re_2(CO)_4(NO)_2(\mu\text{-}Cl)_2(Cl)_2]$ and the phosphines $P((CH_2)_mCH{=}CH_2)_3$ (*m* = 6, **a**; 7, **b**; 8, **c**) give *mer,trans*-$Re(CO)_3(X)(P((CH_2)_mCH{=}CH_2)_3)_2$ (53−95%) or *cis,trans*-$Re(CO)(NO)(Cl)_2(P((CH_2)_6CH{=}CH_2)_3)_2$ (57%), respectively. Additions of Grubbs' catalyst (5−10 mol %, 0.0010−0.0012 M) and subsequent hydrogenations (PtO_2, ≤5 bar) yield the gyroscope-like complexes *mer,trans*-$Re(CO)_3(X)(P((CH_2)_n)_3P)$ (*n* = 2*m* + 2; X = Cl, **7a,c**; Br, **8a,c**; 18−61%) or *cis,trans*-$Re(CO)(NO)(Cl)_2(P((CH_2)_{14})_3P)$ (14%), respectively, and/or the isomers *mer,trans*-$Re(CO)_3(X)(P(CH_2)_{n-1}CH_2)((CH_2)_n)(P(CH_2)_{n-1}CH_2)$ (X = Cl, **7′a−c**; Br, **8′b**; 6−27%). The latter are derived from a combination of interligand and intraligand metatheses. Reactions of **7a** or **8a** with NaI, Ph_2Zn, or MeLi give *mer,trans*-$Re(CO)_3(X)(P((CH_2)_{14})_3P)$ (X = I, **11a**; Ph, **12a**; Me, **13a**; 34−87%). The ^{13}C NMR spectra of **7a−c**, **8a−c**, **11a**, and **13a** show rotation of the $Re(CO)_3(X)$ moieties to be fast on the NMR time scale at room temperature (and at −90 °C for **8a**). In contrast, the phenyl group in **12a** acts as a brake, and two sets of ^{13}C NMR signals (2:1) are observed for the methylene chains. The crystal structures of **7a**, **8a**, **12a**, and **13a** are analyzed with respect to $Re(CO)_3(X)$ rotation in solution and the solid state.

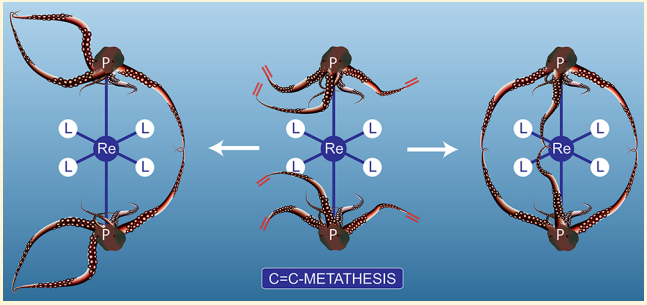

A. INTRODUCTION

Molecular rotors are receiving intensive study from a variety of standpoints,[1−3] and the 2016 Nobel Prize in chemistry has highlighted their application in certain types of molecular machines.[4] We, together with the Garcia-Garibay,[5] Setaka,[6] and other[7] groups, have been particularly interested in rotors that have promise as molecular gyroscopes.[8−14] Here, the rotators are sterically protected to shield neighboring molecules in solution or create a free volume in the solid state. Some typical architectures are shown in Figure 1 (**I**−**III**).

Species of the type **III** have been especially sought in our research group.[8−13] These can be viewed as adducts of metal fragments and dibridgehead diphosphines. They are accessed by threefold intramolecular and interligand ring-closing alkene metatheses of precursors with two *trans* ligands of the formulas $P((CH_2)_mCH{=}CH_2)$ (**IV**), followed by hydrogenations. In a few cases an alternative mixed interligand/*intra*ligand cyclization mode to give **V** can be observed,[9c,12,13] but it is only rarely the dominant product.

We have been examining the efficacy of the threefold ring-closing alkene metatheses as a function of metal coordination geometry and ligand set L_y.[8−13] In previous papers, a variety of trigonal bipyramidal and square planar substrates **IV** (*y* = 2, 3) have been investigated.[8−11] The yields of **III** are, for reasons discussed elsewhere and below, somewhat higher with trigonal bipyramidal complexes.[8,14a] At the outset of this work, we were concerned that octahedral substrates **IV** may present too much steric hindrance for interligand ring-closing metatheses by virtue of the four groups in the equatorial plane.

In this full paper, we describe successful syntheses of octahedral complexes of the type **III**, with $Re(CO)_3(Cl)$, $Re(CO)_3(Br)$, and $Re(CO)(NO)(Cl)_2$ rotators, and attendant spectroscopic, structural, dynamic, and reactivity data. A portion of the results with the first two rotators was communicated earlier.[12] This work is complementary to studies of related complexes with $Os(CO)_2(X)_2$ rotators, which have been detailed separately.[13] Together, these efforts establish the remarkably facile availability of gyroscope-like complexes **III** from precursors

Received: April 9, 2017
Published: June 9, 2017

DOI: 10.1021/acs.inorgchem.7b00909
Inorg. Chem. 2017, 56, 7454−7469

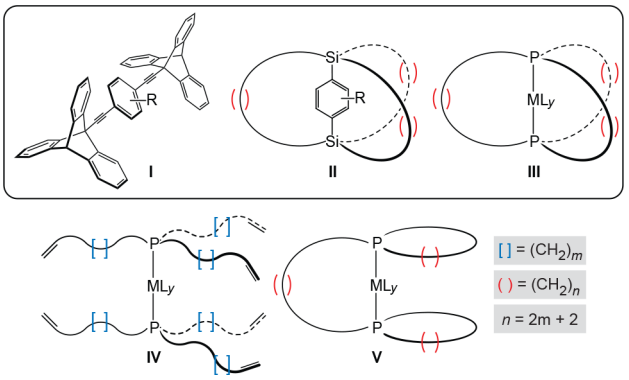

Figure 1. Representative architectures for molecular gyroscopes (**I**–**III**), typical precursors to **III** (**IV**), and occasionally detected byproducts (**V**).

IV that have four small monatomic or linear diatomic ligands in the equatorial plane.

B. RESULTS

B.1. Syntheses of Precursor Complexes. Reactions of the rhenium pentacarbonyl halide complexes $Re(CO)_5(X)$ (X = Cl, Br)[15] and trialkylphosphines PR_3 (2.0 equiv) at elevated temperatures have previously been shown to afford the bis(phosphine) complexes *mer,trans*-$Re(CO)_3(X)(PR_3)_2$.[16] Thus, as illustrated in Scheme 1, reactions of $Re(CO)_5(X)$ with the tris(ω-vinylalkyl)phosphines $P((CH_2)_mCH{=}CH_2)_3$ (m = 6, **1a**; 7, **1b**; 8, **1c**)[17] in chlorobenzene at 140 °C afforded *mer,trans*-$Re(CO)_3(X)(P((CH_2)_mCH{=}CH_2)_3)_2$ (X = Cl, **2a**–**c**; Br, **3a**–**c**). Chromatographic workups gave the chloride complexes **2a**–**c** as yellow oils in 69–95% yields and the bromide complexes **3a**–**c** as orange oils in 53–77% yields.

These new complexes, as well as most others isolated below, were characterized by IR and NMR (^{1}H, ^{13}C{^{1}H}, ^{31}P{^{1}H}) spectroscopy, mass spectrometry, and microanalyses, as detailed in the Experimental Section. Key data are summarized in Table 1. The *mer* relationship of the carbonyl ligands was evidenced by the IR ν_{CO} pattern,[18−20] and a representative spectrum is given in Figure s1 in the Supporting Information. This in turn established a *mer* geometry for the remaining ligands, and the single ^{31}P NMR signal required a *trans* relationship for the two phosphine ligands. This relationship was also evident from the CO ^{13}C NMR signals, which were phosphorus-coupled triplets (ca. 2:1 area ratio corresponding to the two CO ligands *trans* to each other and that *trans* to the halide ligand; see Figure s2). As seen for other complexes of the type **IV** earlier[7−9,11] and illustrated by the representative spectrum in Figure s3, the PCH_2 and $PCH_2CH_2CH_2$ ^{13}C NMR signals were phosphorus-coupled virtual triplets ($^1J_{CP}$ = 13.7–14.4 Hz and $^3J_{CP}$ = 6.1–6.6 Hz),[21] whereas the PCH_2CH_2 signals were singlets. These assignments were verified by ^{1}H,^{1}H COSY, and ^{1}H,^{13}C{^{1}H} COSY NMR spectra of **2a**.

Reactions of the dirhenium tetrachloride tetracarbonyl dinitrosyl complex $[Re_2(CO)_4(NO)_2(\mu\text{-}Cl)_2(Cl)_2]$[22] with trialkylphosphines PR_3 (4.0 equiv) have previously been shown to afford the monorhenium bis(phosphine) complexes *cis,trans*-$Re(CO)(NO)(Cl)_2(PR_3)_2$.[22,23] Thus, as illustrated in Scheme 2, a reaction with **1a** (MeCN, 120 °C) afforded *cis,trans*-$Re(CO)(NO)(Cl)_2(P((CH_2)_6CH{=}CH_2)_3)_2$ (**4a**) as a yellow oil in 57% yield. Consistent with the homologues reported earlier,[22] the IR spectrum showed strong ν_{CO} (1984 cm^{-1}) and ν_{NO} (1718 cm^{-1}) bands. The CO ^{13}C NMR signal was a phosphorus-coupled triplet, indicating a *trans* relationship of the two phosphine ligands, consistent with the single ^{31}P{^{1}H} NMR signal. The chemical shifts and multiplicities of the $PCH_2CH_2CH_2$ ^{13}C NMR signals were similar to those of **2a** and **3a**.

Scheme 1. Syntheses and Ring-Closing Alkene Metatheses of Rhenium Tricarbonyl Halide Complexes 2a–c and 3a–c

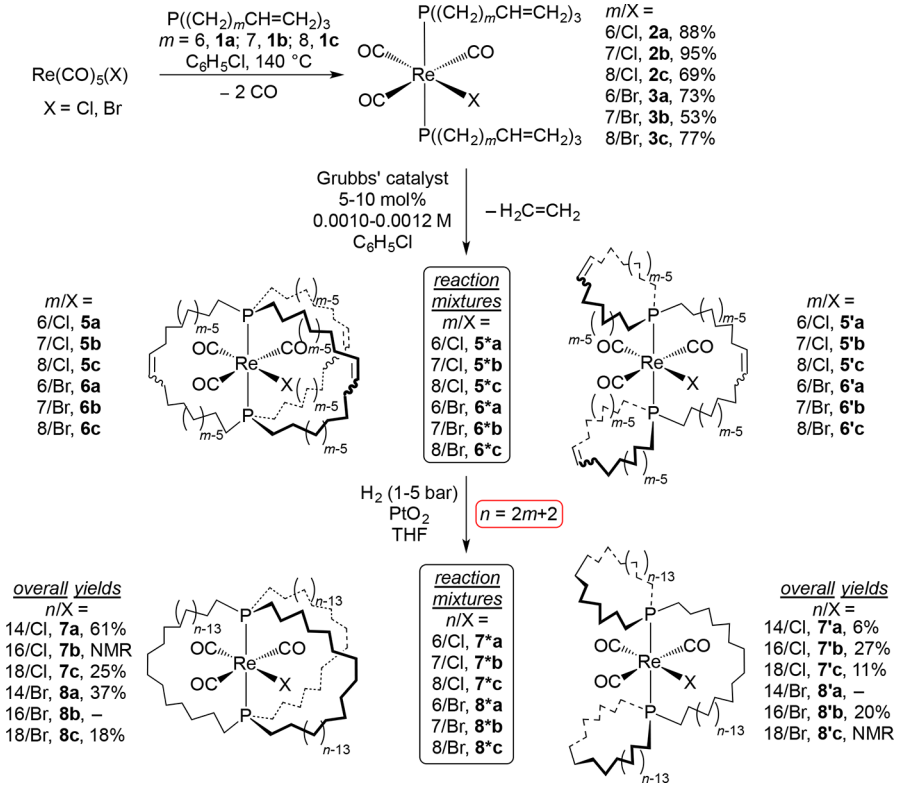

DOI: 10.1021/acs.inorgchem.7b00909
Inorg. Chem. 2017, 56, 7454–7469

Table 1. Selected $^{13}C\{^1H\}$ NMR and IR Data

	$^{13}C\{^1H\}$ (δ/ppm)				
complex	PCH_2 [$^1J_{CP}$, Hz][a]	PCH_2CH_2	$PCH_2CH_2CH_2$ [$^3J_{CP}$, Hz][a]	CO [$^2J_{CP}$, Hz][a,b]	IR (cm^{-1})[c] ν_{CO}, ν_{NO}
2a[d]	27.4 [14.3]	23.9	31.3 [6.1]	195.3 [8.9] 191.8 [6.5]	2026 (w), 1934 (s), 1888 (s)
2b[e]	27.4 [14.3]	23.9	31.4 [6.1]	195.5 [9.0] 192.0 [6.1]	2042 (w), 1930 (s), 1880 (s)
2c[e]	27.5 [13.7]	24.0	31.4 [6.1]	195.5 [8.4] 192.0 [6.1]	2038 (w), 1930 (s), 1884 (s)
3a[e]	27.9 [14.4]	24.0	31.2 [6.6]	194.6 [8.9] 191.5 [6.4]	2026 (m), 1999(m), 1934 (s), 1888 (s)
3b[e]	28.0 [14.3]	24.0	31.3 [6.1]	194.6 [9.1] 191.5 [6.5]	2041 (w), 1930 (s), 1882 (s)
3c[e]	28.0 [14.5]	24.1	31.4 [6.2]	194.7 [9.0] 191.6 [6.5]	2042 (w), 1934 (s), 1888 (s)
4a[e]	23.3 [14.3][f]	23.4	31.3 [6.2]	204.2 [7.0]	1984 (s), 1718 (s)
7a[e]	29.2 [14.4]	23.6	30.4 [6.3]	195.3 [9.0] 191.9 [6.3]	2038 (m), 1922 (s), 1884 (s)
7′a[e]	28.2 [14.8][f,g] 26.7 [13.8][g]	23.8[g] 22.2[g]	30.7 [6.5][g] 28.9 [5.5][g]	195.5 [9.2] 192.0 [6.0]	2038 (w), 1926 (s), 1880 (s)
7′b[e]	28.15 [14.5][f,g] 26.6 [14.0][g]	23.9[g] 23.0[g]	30.9 [6.6][g] 30.1 [5.7][g]	195.5 [9.0] 191.9 [6.1]	2038 (m), 1930 (s), 1880 (s)
7c[e]	27.4 [14.3]	23.5	30.7 [6.0]	195.4 [8.8] 191.8 [6.5]	2038 (w), 1930 (s), 1884 (s)
7′c[e]	28.2 [14.8][g] 26.7 [13.8][g]	24.0[g] 23.3[g]	31.0 [6.5][g] 30.8 [5.5][g]	195.5 [9.2] 192.0 [6.0]	2036 (w), 1927 (s), 1879 (s)
8a[e]	29.9 [14.8]	23.8	30.3 [6.5]	194.6 [8.6] 191.3 [6.3]	2038 (m), 1926 (s), 1884 (s)
8′b[e]	27.2 [13.7][g,h]	24.0[g] 23.1[g]	30.8 [6.7][g] 30.0 [5.8][g]	194.7 [8.7] 191.5 [7.2]	2040 (w), 1930 (s), 1883 (s)
8c[e]	27.9 [14.5]	23.5	30.5 [6.2]	194.6 [8.9] 191.3 [6.0]	2042 (w), 1934 (s), 1888 (s)
9a[e]	24.7 [14.2]	22.4	29.9 [6.5]	203.1 [5.5]	1980 (s), 1718 (s)
10a[e]	29.0 [14.6]	24.2	31.1 [6.1]	193.2 [8.8] 190.6 [6.9]	2038 (w), 1934 (s), 1888 (s)
11a[e]	31.4 [14.7]	24.2	30.3 [6.5]	193.3 [9.3] 190.3 [6.9]	2034 (w), 2011 (w), 1930 (m), 1884 (s)
12a[i]	32.6 [14.2][g] 29.6 [14.5][g]	24.0[g] 22.7[g]	30.4 [6.5][g] 30.1 [6.5][g]	198.2 [9.3] 196.6 [5.6]	2011 (m), 1903 (s), 1876 (s)
13a[e]	30.9–30.3[j]	23.9	30.9–30.3[j]	201.1 [9.2] 195.8 [7.5]	2008 (w), 1900 (m), 1868 (s)

[a]All signals for which J values are given are triplets. [b]In complexes with three CO ligands, the downfield signal corresponds to the two that are *trans*. [c]Oil or powder film; **2a-c** and **3a-c** also give a $\nu_{C=C}$ band (m) at 1640 cm^{-1}. [d]NMR solvent: toluene-d_8. [e]NMR solvent: C_6D_6. [f]One peak of this triplet is obscured; the chemical shift and coupling constant are extrapolated from the two that are visible. [g]Approximate intensity ratio 1:2 (downfield/upfield). [h]The second triplet is obscured by other signals. [i]NMR solvent: CD_2Cl_2. [j]The two triplets overlap and the J values could not be deconvoluted.

Scheme 2. Synthesis and Ring-Closing Alkene Metathesis of Rhenium Carbonyl Nitrosyl Dichloride Complex 4a

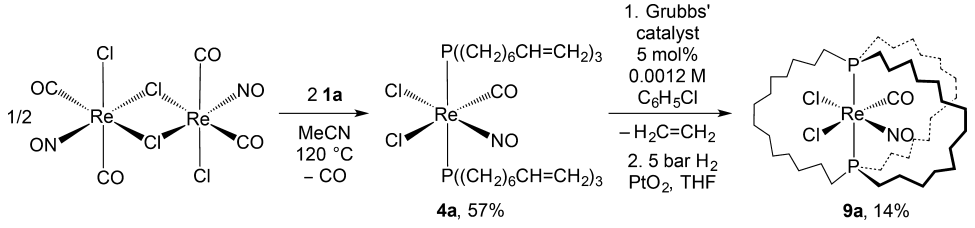

B.2. Syntheses of Title Complexes. As depicted in Scheme 1, ring-closing metatheses of **2a–c** and **3a–c** were performed in dilute chlorobenzene solutions (0.0010–0.0012 M) at room temperature using Grubbs' catalyst (first generation, 5–10 mol %). Nitrogen was aspirated through the samples to purge the coproduct ethene, and aliquots were periodically removed. These were taken up in C_6D_6, and ^1H NMR spectra were recorded. After 21 h, the $CH=CH_2$ signals had been replaced by new CH=CH signals as shown in Figure s4.

DOI: 10.1021/acs.inorgchem.7b00909
Inorg. Chem. 2017, 56, 7454–7469

The samples were filtered through neutral alumina to give the crude metathesis products **5*a–c** (X = Cl; 76–99%) and **6*a–c** (X = Br; 83–90%). As shown in Scheme 1, the target complexes *mer,trans*-$Re(CO)_3(X)(P((CH_2)_mCH{=}CH(CH_2)_m)_3P)$ were designated **5a–c** or **6a–c**. The alternative intramolecular metathesis products *mer,trans*-$Re(CO)_3(X)(P(CH_2)_mCH{=}CH(CH_2)_{m-1}CH_2)((CH_2)_mCH{=}CH(CH_2)_m)(P(CH_2)_mCH{=}CH(CH_2)_{m-1}CH_2)$ were designated **5′a–c** or **6′a–c**. Four C=C isomers are possible for each type of product (*EEE*, *EEZ*, *EZZ*, *ZZZ*). Accordingly, $^{31}P\{^1H\}$ NMR spectra exhibited at least four principal signals, as illustrated in Figure s5.

The mixtures **5*a–c** and **6*a–c** were treated with 1–5 bar of H_2 in the presence of the catalyst PtO_2 (10 mol %). In all cases, ^1H NMR spectra of aliquots taken after 1–2 d showed complete CH=CH consumption. Workups gave the samples designated **7*a–c** or **8*a–c** in Scheme 1. Note that these carry the new indices *n*, signifying the number of methylene groups in each *trans* spanning linkage ($n = 2m + 2$). For **7*a**, the $^{31}P\{^1H\}$ NMR spectrum showed one main signal and two much less intense upfield signals (Figure s6). With **7*b**, the dominant signal was upfield, with a less intense one downfield (3.6:1). With **7*c**, the dominant signal was again downfield, with a less intense one upfield (2:1).

The samples **7*a–c** and **8*a–c** were chromatographed. With **7*a,c**, both the gyroscope-like complexes **7a,c** (61%, 25%; all yields from acyclic precursors **2a–c** or **3a–c**) and the isomeric non-gyroscope species **7′a,c** (8%, 11%) could be isolated. The $^{31}P\{^1H\}$ NMR signals of the former were downfield of the latter. In the case of **7*b**, only the isomeric species **7′b** proved isolable (28%), although it is believed that the other (downfield) ^{31}P signal noted above can be assigned to **7b**. In the cases of **8*a–c**, selectivities appeared somewhat higher. With **8*a**, only **8a** was detected by $^{31}P\{^1H\}$ NMR and subsequently isolated (37%). With **8*b**, only **8′b** was detected by $^{31}P\{^1H\}$ NMR and subsequently isolated (20%). With **8*c**, substantial amounts of **8c** and trace amounts of **8′c** were apparent, but only **8c** was subsequently isolated (18%).

As shown in Scheme 2, the carbonyl nitrosyl dichloride complex **4a** was analogously elaborated with the help of NMR monitoring to a crude metathesis product. Subsequent hydrogenation gave the gyroscope-like complex **9a** in 14% overall yield.

The structures of several of these gyroscope-like complexes have been confirmed crystallographyically (vide infra). However, $^{13}C\{^1H\}$ NMR spectra also played decisive roles in the assignments. Specifically, the non-gyroscope complexes gave two sets of $n/2$ methylene signals in a ca. 2:1 area ratio, as illustrated in Figure s7. The more intense set can be attributed to the two macrocycles derived from *intra*ligand metathesis. The less intense set corresponds to the *trans* spanning methylene chain derived from *inter*ligand metathesis. In contrast, the gyroscope-like complexes gave a single set of $n/2$ methylene signals, consistent with $Re(CO)_3(Cl)$ or $Re(CO)_3(Br)$ rotation being fast on the NMR time scale. These dynamic properties are treated in more detail below.

Complexes **7a**, **8a**, and **9a** were isolated as white powders with high melting points (230–278 °C), whereas **7c** and **8c** were pale yellow oils. Complex **7′a** was a white, iridescent, lower-melting powder (70 °C); **7′b,c** were pale yellow oils, and **8′b** was a sticky white oil. In general, complexes of the type **V** are less crystalline than the analogous gyroscope-like complexes **III**. Differential scanning calorimetry (DSC) and thermogravimetric analysis (TGA) data were obtained for several compounds,[24] and are summarized in Table s1 (Supporting Information).

B.3. Substitution Reactions. Rhenium carbonyl or nitrosyl halide complexes have been shown to undergo a variety of substitution reactions.[25,26] As depicted in Scheme 3, the acyclic

Scheme 3. Substitution Reactions with NaI

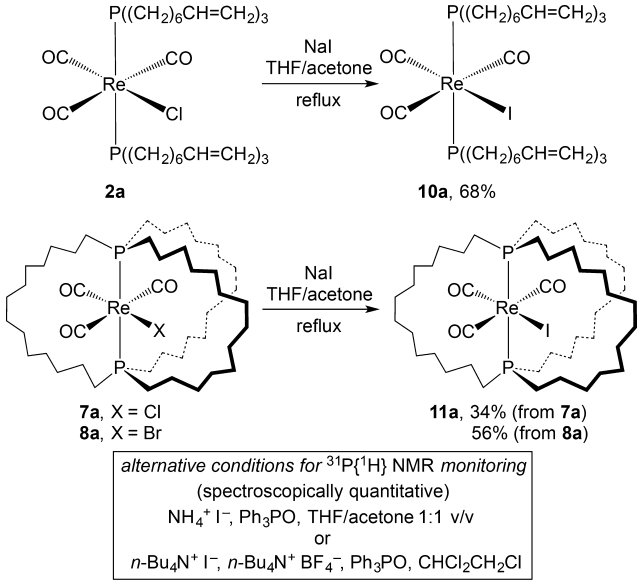

precursor complex **2a** and the gyroscope-like complexes **7a** and **8a** were combined with NaI in refluxing tetrahydrofuran (THF)/acetone (2:1 v/v). With the chloride complexes **2a** and **7a**, $^{31}P\{^1H\}$ NMR spectra showed greater than 99% consumption after 20–25 h. With the bromide complex **8a**, one week was required. Workups gave the iodide complexes *mer,trans*-$Re(CO)_3(I)(P((CH_2)_6CH{=}CH_2)_3)_2$ (**10a**) as a yellow oil in 68% yield, and *mer,trans*-$Re(CO)_3(I)(P((CH_2)_n)_3P)$ (**11a**) as a pale yellow powder in 34–56% yields.

As shown in Scheme 4, the halide ligands of **7a** and **8a** could also be substituted by carbon nucleophiles. A THF solution of **7a** and Ph_2Zn was refluxed for 2 d. Workup gave the phenyl complex *mer,trans*-$Re(CO)_3(Ph)(P((CH_2)_n)_3P)$ (**12a**) as an orange powder in 87% yield. Similar reactions were performed with **7a** or **8a** and MeLi. Workups gave the methyl complex **13a** as a white powder in yields from 78% (after 1 d from **7a**) to 82% (after 2 d from **8a**). Substitution reactions have been successfully performed with sulfur and other carbon nucleophiles, but the products have only been partially characterized.[27] Attempts to effect CO/NO^+ substitutions with nitrosonium salts such as NO^+ BF_4^- have been unsuccessful.[27]

In contrast to all of the preceding gyroscope-like complexes with $P(CH_2)_{14}P$ linkages, the $^{13}C\{^1H\}$ NMR spectrum of the phenyl complex **12a** showed 14 CH_2 signals. These consisted of two sets of seven with a ca. 2:1 area ratio. A crystal structure (below) excludes an isomeric complex of the type **V**. Hence, this phenomenon is attributed to the slow rotation of the $Re(CO)_3(Ph)$ rotator on the NMR time scale, resulting in one $(CH_2)_{14}$ segment that does not readily exchange with the other two. This is further treated in the discussion of dynamic properties below.

For all of the substitution products, the $PCH_2CH_2CH_2$ $^{13}C\{^1H\}$ NMR signals exhibited chemical shift and coupling

DOI: 10.1021/acs.inorgchem.7b00909
Inorg. Chem. 2017, 56, 7454–7469

Scheme 4. Substitution Reactions with Carbon Nucelophiles

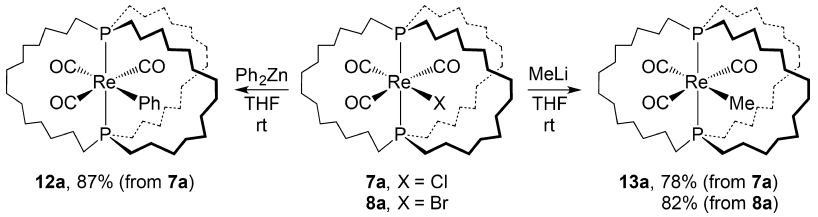

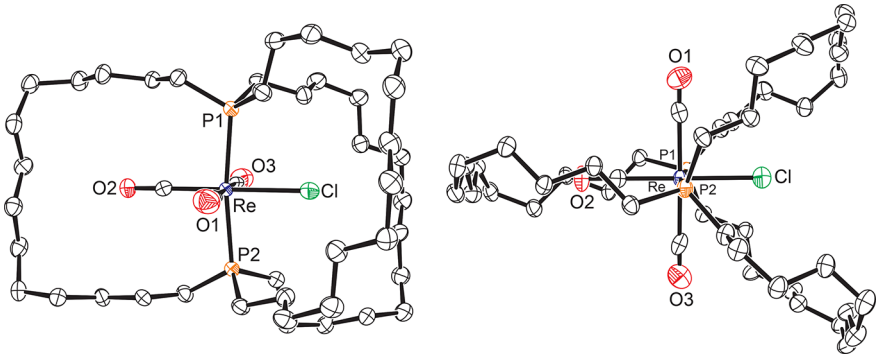

Figure 2. Thermal ellipsoid plots of **7a** with the P−Re−P axis in (left) and perpendicular to (right) the plane of the paper.

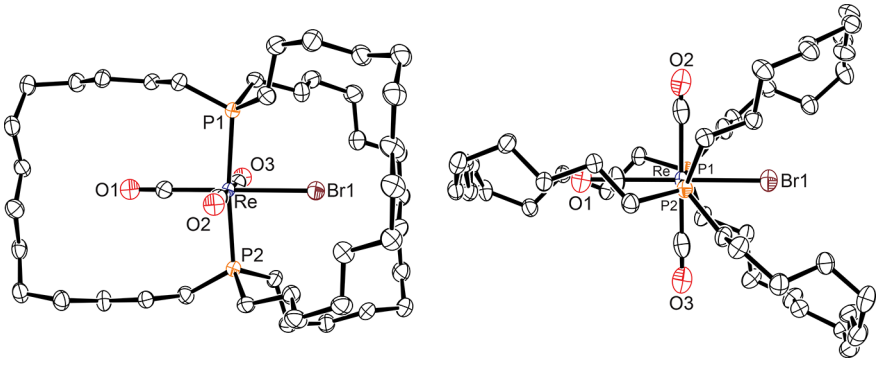

Figure 3. Thermal ellipsoid plots of the dominant rotamer of **8a** with the P−Re−P axis in (left) and perpendicular to (right) the plane of the paper.

constant patterns analogous to those of their precursors. The methyl complex **13a** afforded $ReCH_3$ ^1H and $^{13}C\{^1H\}$ NMR signals at −0.27 and −31.9 ppm, respectively; each was a triplet due to phosphorus coupling. Similar upfield chemical shifts have been observed with other rhenium methyl complexes.[26a,28]

Scout experiments were conducted to lay the groundwork for rate studies. It has been a long-standing goal to compare the rate laws for substitution reactions of gyroscope-like complexes such as **7a** with those of acyclic analogues such as **2a**. As summarized in Scheme 3, homogeneous conditions suitable for NMR tube-scale experiments could be developed for the conversions of **2a** and **7a** to iodide complexes **10a** and **11a** (NH_4^+ I^- or *n*-Bu_4N^+ I^- in THF/acetone or 1,1,2-trichloroethane with a Ph_3PO internal standard). However, the reactions in THF/acetone were still quite slow near the boiling point of the solvent, and some decomposition appeared to occur in the higher-boiling 1,1,2-trichloroethane. Nonetheless, the consumption of **2a** was moderately faster than that of **7a** under all conditions investigated.

B.4. Structural and Dynamic Properties. Structural data were sought for as many complexes as possible. Crystals of the gyroscope-like complexes **7a**, **8a**, **12a**, and **13a** (or solvates thereof) could be grown, but efforts with isomeric non-gyroscope species (**V**) were unsuccessful. X-ray data were acquired (173.15 K), and the structures were solved as outlined in Table s2 and the Experimental Section. Thermal ellipsoid diagrams are collected in Figures 2 to 5. These data confirmed the assigned structures, including the *mer,trans* stereochemistry. Metrical parameters are summarized in Tables 2 (various types of distances) and s3 (various types of angles). The bond lengths and angles were very similar to those in related octahedral rhenium carbonyl chloride, bromide, phenyl, and methyl complexes, some references for which are given in the Supporting Information.

The chloride complex **7a** and bromide complex **8a** crystallized in nearly identical lattices, as illustrated by the data in Table s2 and elaborated further below. However, the bromide and two carbonyl ligands in **8a**, unlike the chloride and carbonyl ligands in **7a**, were disordered. As shown in Figures 2 and 3, one carbonyl ligand occupied the center "hole" of one 17-membered macrocycle. For **7a**, the chloride ligand was always *trans* to this carbonyl ligand. With **8a**, the bromide ligand was found in all three remaining positions, but predominantly *trans* to the carbonyl ligand in the hole (70:15:15 occupancy ratio after refinement). Figure 3 depicts only the dominant rotamer, whereas an overlay of all three is given in Figure s10.

The unit cell of the monosolvated phenyl complex **12a**·THF featured four independent molecules, as illustrated in Figure 4.

DOI: 10.1021/acs.inorgchem.7b00909
Inorg. Chem. 2017, 56, 7454−7469

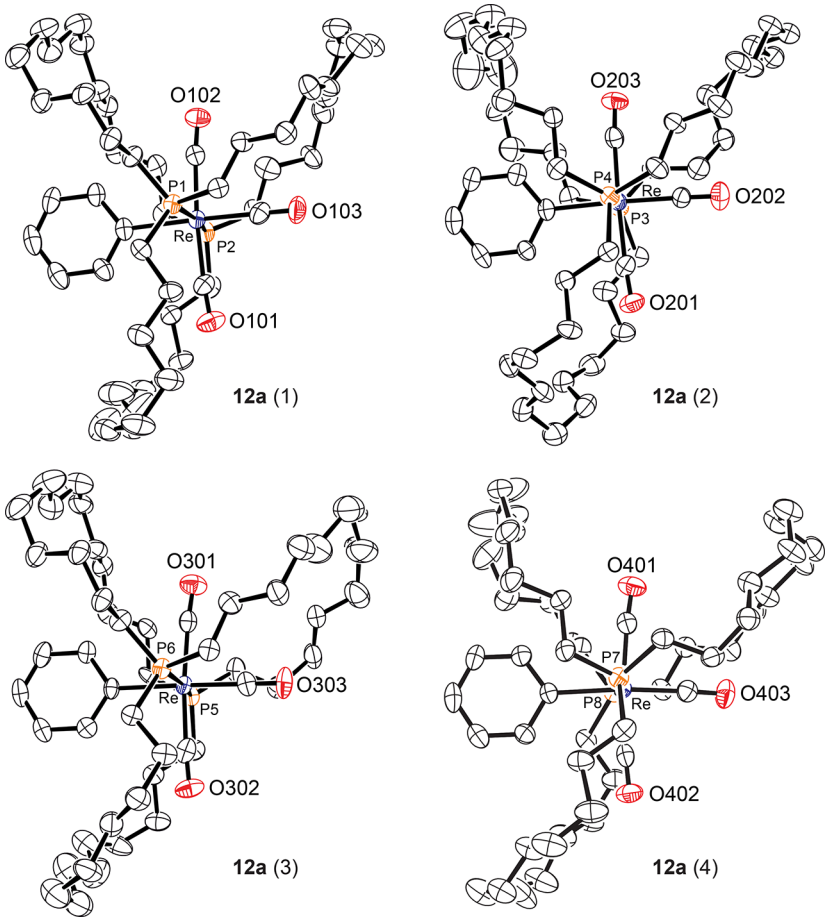

Figure 4. Thermal ellipsoid plots of the four independent molecules of **12a** in the unit cell of **12a**·THF with the P−Re−P axes perpendicular to the plane of the paper (the molecule numbering corresponds to the data in Table 2).

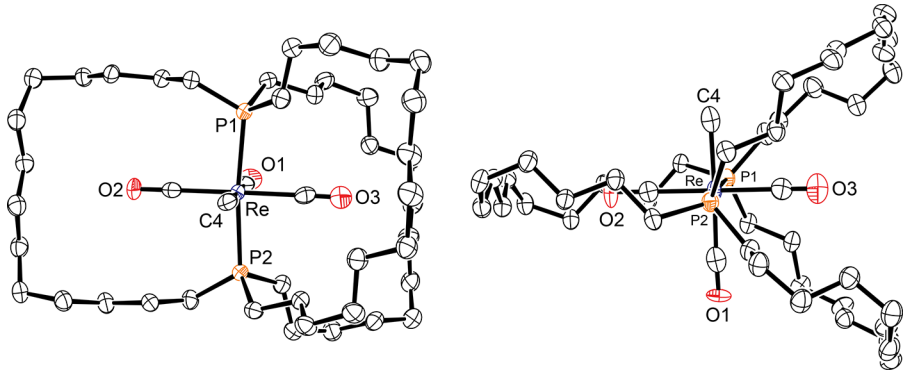

Figure 5. Thermal ellipsoid plots of dominant rotamer of **13a** with the P−Re−P axis in (left) and perpendicular to (right) the plane of the paper.

These exhibited minor differences in the macrocycle conformations. Note that in some of these perspectives, the macrocycle arrays are more "T" shaped than "Y" shaped. The methyl complex **13a** crystallized in a lattice very similar to those of **7a** and **8a**. Again, as shown in Figure 5, one carbonyl ligand occupied the center hole of one 17-membered macrocycle. The methyl ligand was disordered over the two positions *cis* to this carbonyl ligand (55:45 after refinement).

As implied in passing above, **7a**, **8a**, and **13a** crystallized in identical space groups ($P2_1/n$) and with very similar lattice constants (Z = 4, V = 4739.02(19)−4767.78(18) Å^3) and macrocycle conformations (Figures 2, 3, 5). In each case there are two sets of molecules with parallel P−Re−P axes, but with a nonparallel relationship to each other, as illustrated in Figure 6. Several approaches have been used to calculate the angles between the nonparallel axes.[9c,13a,14a] The most intuitive is to define one least-squares plane consisting of the six atoms of two parallel P−Re−P axes of one set, and an analogous least-squares plane of the other set (planes defined by only three nearly collinear experimental points tend to have large error limits). The resulting angles are 30.4° (**7a**), 34.6° (**8a**), and 32.9° (**13a**). Unsurprisingly given Figure 4, **12a** crystallizes in a more complicated lattice, with four sets of molecules with parallel P−Re−P axes.

The gyroscope-like molecules were probed for dynamic behavior. For example, $^{13}C\{^1H\}$ NMR spectra of the bromide

DOI: 10.1021/acs.inorgchem.7b00909
Inorg. Chem. 2017, 56, 7454−7469

Table 2. Key Interatomic Distances Involving Gyroscope-like Complexes [Å]

	7a	8a[a]	12a(1)[b]	12a(2)[b]	12a(3)[b]	12a(4)[b]	13a[a]
Re−P	2.4266(8)	2.4300(9)	2.4230(16)	2.4219(16)	2.4194(15)	2.4270(15)	2.4113(9)
	2.4297(8)	2.4300(8)	2.4289(16)	2.4223(15)	2.4357(16)	2.4372(15)	2.4120(9)
P to P	4.844	4.850	4.833	4.836	4.834	4.842	4.815
C−O	1.046(4)	1.099(4)	1.124(7)	1.141(7)	1.149(7)	1.127(7)	1.088(6)
	1.121(4)	0.844(5)	1.156(7)	1.173(6)	1.141(7)	1.137(7)	1.129(4)
	1.019(4)	1.087(5)	1.149(6)	1.140(7)	1.159(6)	1.157(6)	1.055(5)
Re-CO	2.037(4)	2.116(5)	2.003(6)	1.976(6)	1.968(6)	1.992(6)	2.077(5)
	1.922(4)	1.957(3)	1.970(6)	1.930(5)	1.986(7)	1.989(6)	1.975(4)
	2.054(4)	1.996(5)	1.949(6)	1.973(6)	1.935(5)	1.940(5)	2.003(4)
average Re−CO	3.066	3.032	3.115	3.109	3.110	3.112	3.109
Re−CO_{rotor}[c]	4.59	4.55	4.64	4.63	4.63	4.63	4.63
Re−X[d]	2.531(10)	2.6596(7)	2.245(5)/6.035	2.215(5)/6.041	2.227(5)/6.039	2.224(5)/6.044	2.119(5)
Re−X_{rotor}[e]	4.28	4.51	7.24	7.24	7.24	7.24	3.82
	7.252/6.587	7.214/6.544	6.783/7.076	6.585/7.341	6.804/7.275	7.094/6.789	7.230/6.559
Re−C_{dis}[f]	6.563/7.248	6.578/7.243	6.645/6.754	7.441/6.944	6.525/7.310	6.823/7.207	6.590/7.257
	6.579/6.579	6.577/6.584	7.436/7.179	7.554/6.957	7.066/6.767	7.311/6.781	6.584/6.588
shortest/longest Re−C_{dis}−vdW[g]	4.86/5.55	4.84/5.54	4.95/5.74	4.89/5.85	4.83/5.61	5.08/5.61	4.86/5.58
Re−C_{inter}[h]	5.122	5.167	5.418	5.487	5.353	5.278	5.172
Re−C_{inter}−vdW[i]	3.42	3.47	3.72	3.79	3.66	3.58	3.47

[a]Values for the dominant $Re(CO)_3(Br)$ (**8a**) or $Re(CO)_3(Me)$ (**13a**) rotamer. [b]Values for the four independent molecules of **12a** in the unit cell (THF monosolvate). [c]The average rhenium−oxygen distances plus the van der Waals radius of oxygen (1.52 Å). [d]X = Cl, Br, C_{ipso}/H_{para} or CH_3. [e]The Re-X distance plus the van der Waals radius of X (Cl, 1.75 Å; Br, 1.85 Å; H 1.20 Å, C, 1.70 Å). [f]Distances from rhenium to the two carbon atoms of each macrocycle that are closest to the plane of the rotator (C_{dis}). [g]The shortest/longest of the previous six distances, minus the van der Waals radius of carbon (1.70 Å). [h]Distance from rhenium to the nearest non-hydrogen atom of a neighboring molecule (always a carbon atom). [i]The previous entry minus the van der Waals radius of carbon (1.70 Å).

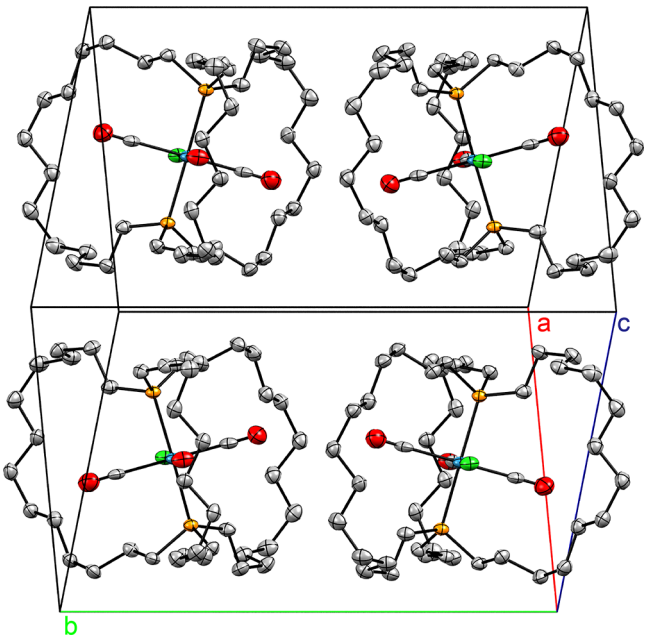

Figure 6. Unit cell of chloride complex **7a**.

complex **8a** were recorded in toluene-d_8 at 20 °C and then at 10−20 °C intervals down to −100 °C. Special attention was given to the CH_2 signals that decoalesce in trigonal bipyramidal analogues.[8,14a] However, the peaks simply broadened and/or became less intense, perhaps due to partial precipitation. Complex **7a**, with the smaller chloride ligand, would be certain to have a lower rotational barrier than **8a**. Hence, even lower decoalescence temperatures would be expected.

Interestingly, the DSC trace of **7a** showed a significant endotherm at 41 °C (Table s1), far below the melting point (230 °C). This phenomenon was probed by X-ray crystallography; a data set was collected at 50 °C. The temperature dependence of the shapes of thermal ellipsoids has in some cases been correlated to rotational barriers.[29] The new data set was solved and revealed no new disordered atoms or phase transitions versus the low-temperature data set obtained above. However, the quality of the crystal diminished, and no quantitative analyses were undertaken.

C. DISCUSSION

C.1. Scope of Syntheses. Additional observations provide further context for the successful syntheses of octahedral gyroscope-like complexes in Schemes 1 and 2. First, analogues of **2a−c** and **3a−c** were prepared but with only four or five methylene groups in each substituent of the ligand $P((CH_2)_mCH{=}CH_2)_3$ (i.e., m = 4 or 5).[27,30] When these were similarly treated with Grubbs' catalyst, no fully cyclized monorhenium products could be detected. Even with longer reaction times and higher temperatures and catalyst loadings, the terminal $CH{=}CH_2$ linkages were only partially consumed. In contrast, the analogous trigonal bipyramidal iron complexes *trans*-$Fe(CO)_3(P((CH_2)_mCH{=}CH_2)_3)_2$ (m = 4, 5) underwent efficient intramolecular alkene metatheses to give (after hydrogenations) complexes of the type **III** in 50−63% yields.[8a,b] Thus, the formation of octahedral gyroscope-like complexes requires at least six methylene groups in each phosphine ligand substituent of the precursor **IV**.

Results very similar to those in Scheme 1 have been obtained with octahedral osmium dicarbonyl dichloride and dibromide complexes, *cis,cis,trans*-$Os(CO)_2(X)_2(P((CH_2)_mCH{=}CH_2)_3)_2$ (X = Cl, **14a−c**; X = Br, **15a−c**).[13a] These are summarized in Scheme 5. Importantly, the structure of the non-gyrosocope species **19a** (n/X = 14/Br) could be confirmed crystallographically. The distribution of gyroscope-like versus non-gyroscope products (**III**/**V**) parallels that with the rhenium complexes. In both cases,

DOI: 10.1021/acs.inorgchem.7b00909
Inorg. Chem. 2017, 56, 7454−7469

Scheme 5. Metathesis/Hydrogenation Sequences with Octahedral Osmium Complexes

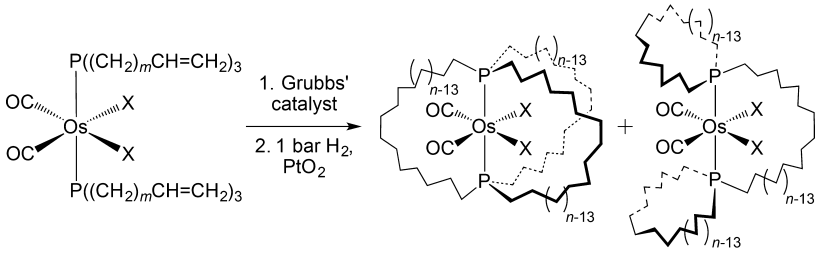

m/X = 6/Cl, **14a**	*n*/X = 14/Cl, **16a**, 28%	*n*/X = 14/Cl, **18a**, 13%
7/Cl, **14b**	16/Cl, **16b**, 5%	16/Cl, **18b**, 51%
8/Cl, **14c**	18/Cl, **16c**, 23%	18/Cl, **18c**, 12%
6/Br, **15a**	14/Br, **17a**, 31%	14/Br, **19a**, 18%
7/Br, **15b**	16/Br, **17b**, 5%	16/Br, **19b**, 40%
8/Br, **15c**	18/Br, **17c**, 27%	18/Br, **19c**, 24%

precursor complexes with even numbers of methylene groups in each phosphorus substituent (i.e., **2a,c**, **3a,c**, **14a,c**, **15a,c**) afford mainly **III**. Complexes of the one phosphine with an odd number of methylene groups in each substituent (i.e., **2b**, **3b**, **14b**, **15b**) afford mainly **V**. To date, we lack a rationale for this strong dependence of product type upon the methylene chain length. Although more examples are needed to rigorously establish an even/odd selectivity correlation, there is abundant precedent for the alternation of molecular properties with even/odd counts of methylene groups.[31]

Among other successful approaches, Setaka was able to access the disilicon gyroscope-like molecules **II** (Figure 1) via three-fold intramolecular ring-closing metatheses of the precursors *p*-$(H_2C{=}CH(CH_2)_m)_3SiC_6H_4Si((CH_2)_mCH{=}CH_2)_3$.[6b,c] He also encountered isomeric byproducts analogous to **V**, and the ratios were similarly strong functions of the number of methylene groups *m* (6, 24:0; 7, 10:43; 8, 23:39).[6b] Both types of products were also observed with other arene rotators.[6a,d−f] Setaka noted that if all $CH{=}CH_2/CH{=}CH_2$ combinations undergo metathesis at identical rates, non-gyroscope products should dominate over gyroscope-like products (3:1).[6c]

Although the yields of most of the octahedral gyroscope-like complexes in Schemes 1, 2, and 5 are modest, that of the chloride complex **7a** (61%) stands out. In view of the lower yield of the bromide analogue **8a** (37%), this is tentatively interpreted as a ligand size effect. The lower yields versus those realized with trigonal bipyramidal precursors *trans*-$Fe(CO)_3(P((CH_2)_mCH{=}CH_2)_3)_2$ can be rationalized from the conformational models in Figure 7 (top). In ML_3 adducts, the three $(CH_2)_mCH{=}CH_2$ substituents on each phosphorus atom will prefer to be staggered relative to the three ligands on the metal, as shown in **VI**. This preorganizes the phosphine substituents for intramolecular and interligand alkene metathesis. In contrast, there are no such synergies in octahedral ML_4 adducts. One or two of the metal-based ligands will be nearly eclipsed with the $(CH_2)_mCH{=}CH_2$ substituents on phosphorus, as shown in **VII**. Hence, intermolecular and intraligand alkene metatheses should be better able to compete.

Other octahedral gyroscope-like complexes have been synthesized via additions to trigonal bipyramidal or square planar precursors. As shown in Scheme 6 (top), adducts with $Fe(CO)_3$ rotators (**20**) are easily protonated to give cationic $[Fe(CO)_3(H)]^+$ species.[8a,b] Alternatively, oxidative additions can be conducted with square planar Rh(CO)(X) species, as exemplified for **22** in Scheme 6 (bottom).[11a] Since the ligands on the rotator in product **23** are unlike, and the CCl_3 ligand is too large to pass through a 17-membered macrocycle (see next section),

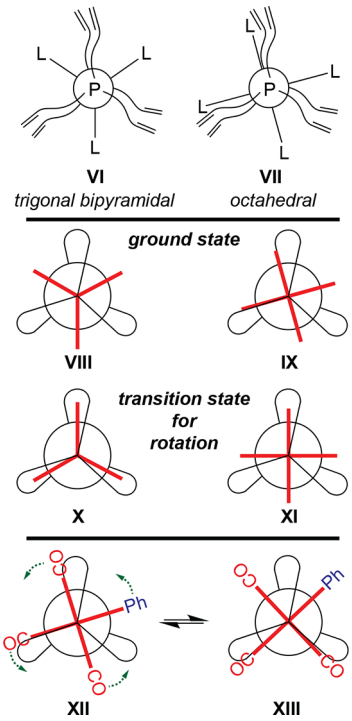

Figure 7. (top) **VI**, preorganization of ligands prior to ring-closing metathesis of a trigonal bipyramidal precursor to gyroscope-like complexes **III**; **VII**, pell-mell disposition of ligands in an analogous octahedral precursor. (middle) Ground-state conformations of trigonal bipyramidal (**VIII**) and octahedral (**IX**) gyroscope-like complexes **III**, and the respective transition states for rotator rotation (**X**, **XI**). (bottom) Mirror image rotator conformations of phenyl complex **12a**.

the $^{13}C\{^1H\}$ NMR spectrum exhibits three sets of $(CH_2)_{n/2}$ signals ($n = 7$).

C.2. Structural and Dynamic Properties. The crystallographic data provide a framework for analyzing the barriers to $Re(CO)_3(X)$ rotation. The initial step is to establish the radius of the rotator, each of which will have a "radius determining" ligand as highlighted in Figure 8. For example, the average rhenium−oxygen (ReCO) distances in **7a**, **8a**, and **13a** range from 3.032 to 3.109 Å (Table 2).[32] When the van der Waals radius of an oxygen atom is added (1.52 Å),[33] values of 4.55 to 4.63 Å for the effective ReCO radius are obtained.

The rhenium−chloride, −bromide, and −methyl distances in **7a**, **8a**, and **13a** are somewhat shorter (2.53, 2.66, and 2.12 Å). When the van der Waals radii of the halide or methyl carbon

DOI: 10.1021/acs.inorgchem.7b00909
Inorg. Chem. 2017, 56, 7454−7469

Scheme 6. Alternative Approaches to Octahedral Gyroscope-like Complexes

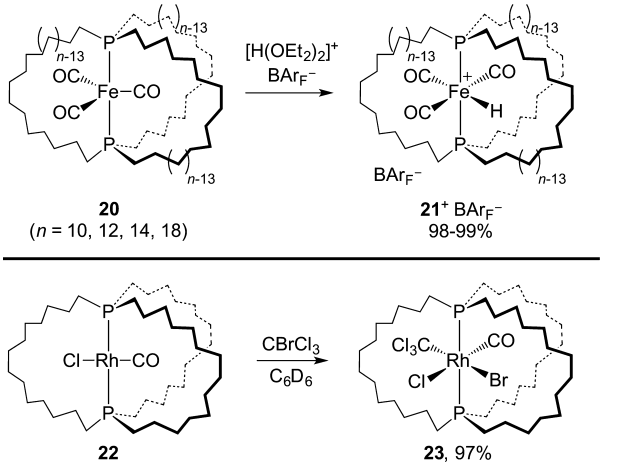

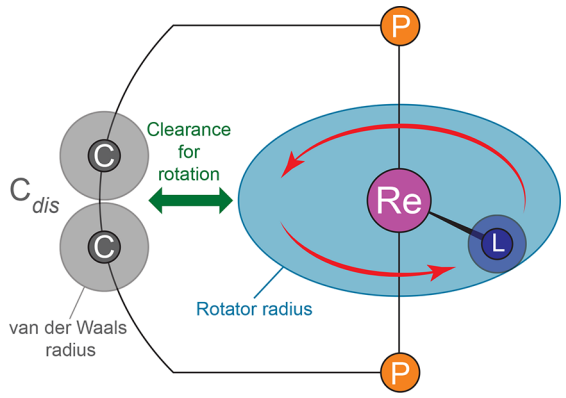

Figure 8. Some spatial relationships in the title compounds involving the rotators and methylene carbon atoms connecting the *trans* phosphorus atoms.

atom are added (1.75, 1.85, and 1.70 Å),[33] slightly lower values are obtained (4.28, 4.51, and 3.82 Å). Hence, the effective radius of the rotator in **7a**, **8a**, and **13a** can be taken as 4.55 to 4.63 Å. In the case of the phenyl complex **12a**, analysis is complicated by the four independent molecules in the unit cell. Nonetheless, it is obvious that the phenyl ligand will be radius-determining. Hence, the distances from the rhenium atoms to the *para* hydrogen atoms (6.035, 6.041, 6.039, 6.044 Å) are averaged (6.04 Å), and the van der Waals radius of a hydrogen atom is added (1.20 Å). This gives an effective radius of 7.24 Å.[34]

As illustrated in Figure 8, distances can also be calculated from the rhenium atom to the remote carbon atoms of the macrocycle that are closest to the plane of the rotator—which are often but not always the two carbon atoms in the middle of the methylene chain. The six values associated with each complex are listed in Table 2. The van der Waals radius of a carbon atom is then subtracted from the shortest distance.[35] This gives a minimum "horizontal clearance" of 4.83−5.08 Å, which comfortably accommodates the radii of the rotators of the chloride, bromide, and methyl complexes **7a**, **8a**, and **13a**. However, the radius of the rotator of the phenyl complex **12a** is clearly too great to pass through a macrocycle, in accord with the ^{13}C NMR data noted above.

Additional issues affect rotational barriers. One is the vertical or top/bottom clearance. It can easily be shown that the van der Waals *diameters* of the chloride and bromide atoms (3.50 and 3.70 Å)[33] exceed the free volume within the $\underline{C}H_2$−P−Re−P−$\underline{C}H_2$ segments of the diphosphine cages. For a more detailed analysis of these interactions, readers are referred to a study that compares analogous diphosphine and diarsine complexes.[14a] The As−M−As distances are ca. 3−4% greater than the P−M−P distances, affording significantly decreased barriers. Another issue, applicable to barriers in the crystal lattice, involves the distance from rhenium to the nearest non-hydrogen atom of a neighboring molecule. When this value, adjusted for the van der Waals radius of the nearest atom, is greater than the radius of the rotator, there is no intermolecular impediment to rotation of the rotator. As summarized in Table 2, all of these distances (Re/C_{inter}-vdW) are much shorter than the radii of the rotators, rendering solid-state rotation infeasible.

Other considerations are relevant to the surprisingly facile $Re(CO)_3(X)$ rotation in **7a**, **8a**, and **13a**. As depicted in Figure 7 (middle), the transition states for ML_3 rotation in trigonal bipyramidal complexes (e.g., **20**, Scheme 6) feature a threefold eclipsing interaction as shown in **X**. Naturally, this should be much higher in energy than the staggered ground-state **VIII**. In contrast, the octahedral complexes **7a**, **8a**, and **13a** would all have singly eclipsed transition states as shown in **XI**. However, nearly eclipsed groups cannot be avoided in the ground-state **IX** due to the higher coordination number. These destabilizing interactions should raise the ground-state energy versus that of **VIII** and lessen the rotational barriers in the octahedral complexes. Said differently, the octahedral complexes feature 12-fold rotational barriers (12 energy maxima and 12 minima in the course of a 360° rotation), whereas the trigonal bipyramidal complexes feature threefold rotational barriers (three maxima and three minima). It is an established physical organic principle that higher-order rotational barriers must be (considerably) less than lower-order rotational barriers when they involve substituents of comparable sizes.[36]

The ground-state conformation of the phenyl complex **12a** deserves special attention in view of the $^{13}C\{^1H\}$ NMR spectrum (two sets of seven CH_2 signals, ca. 2:1 area ratio). Consistent with the solid-state structures in Figure 4, the larger phenyl group would logically prefer the middle region of the interstice between the two neighboring 17-membered macrocycles, as depicted in **XII** (Figure 7, bottom). However, the three macrocycles are inequivalent in **XII**, and *three* sets of seven CH_2 signals in a ca. 1:1:1 area ratio would be expected. Importantly, the $^{13}C\{^1H\}$ NMR spectra of **7a**, **8a**, and **13a** (one set of seven CH_2 signals) establish, in line with geometric considerations above, that the carbonyl ligands can easily rotate through 17-membered macrocycles. Thus, **XII** should be able to equilibrate with the mirror image **XIII** by a 30° $Re(CO)_3(Ph)$ rotation. This exchanges the two macrocycles that neighbor the phenyl group, accounting for the two sets of signals and their relative intensities.

Finally, one other type of dynamic property deserves mention. An increasingly popular technique, "ion mobility mass spectrometry", interrogates the gas-phase diffusivities and collisional cross sections of positive ions.[37] When the molecular ions of complexes of the types **III** and **V** are compared—as specifically done for **7a** and **7′a** (Scheme 1) and several analogous pairs of complexes from Scheme 5—those derived from ovoid-shaped **III** travel considerably faster through a drift chamber containing a low pressure of a neutral buffer gas (nitrogen) than the less compact **V**.[13b] Only very small sample sizes are required for such determinations, and the sensitivity can be greater that that for a popular assay of diffusivity in solution, DOSY NMR.

DOI: 10.1021/acs.inorgchem.7b00909
Inorg. Chem. 2017, 56, 7454−7469

C.3. Summary. Octahedral gyroscope-like complexes that feature tetrasubstituted $Re(CO)_3(Cl)$, $Re(CO)_3(Br)$, and $Re(CO)(NO)(Cl)_2$ rotators encased within triply spoked $P((CH_2)_n)_3P$ (n = 14, 16, and 18) stators are easily prepared by ring-closing interligand alkene metatheses and hydrogenations of precursors with two *trans* ligands of the formulas $P((CH_2)_mCH{=}CH_2)$ ($n = 2m + 2$). The halide ligands can be substituted by nucleophiles such as NaI, Ph_2Zn, and MeLi. Except for the $Re(CO)_3(Ph)$ species with n = 14, rotation about the P−Re−P axis is facile in solution, as established by NMR and in accord with geometric considerations derived from crystallographic data. Isomeric species derived from a combination of *inter*ligand and *intra*ligand alkene metathesis are also often produced. When n = 16, these are the major products.

D. EXPERIMENTAL SECTION

General Data. ^1H, $^{13}C\{^1H\}$, and $^{31}P\{^1H\}$ NMR spectra were recorded on standard 300−400 MHz spectrometers at ambient probe temperatures and referenced as follows (δ, ppm): ^1H, residual internal C_6D_5H (7.15) or $CDHCl_2$ (5.23); ^{13}C, internal C_6D_6 (128.0), toluene-d_8 (137.4, 128.9, 128.0, 125.1, 20.5), or CD_2Cl_2 (53.5); ^{31}P, external H_3PO_4 (0.00). Fourier transform infrared (FT IR) spectra were recorded using ASI React-IR 1000 or Thermo Scientific Nicolet IR100 spectrometers. Mass spectra were obtained using Micromass Zabspec and Shimadzu Biotech Axima Confidence instruments. Melting points were determined on an Electrothermal IA 9100 apparatus or a Stanford Research Systems (SRS) MPA100 (Opti-Melt) automated device. DSC and TGA data were recorded with a Mettler-Toledo DSC821 instrument and treated by standard methods.[24] Microanalyses were conducted on a Carlo Erba EA1110 instrument (in house).

Except for hydrogenations, reactions were conducted under dry N_2 atmospheres. Chromatographies were conducted in air. Reaction solvents were treated as follows: THF, distilled from Na/benzophenone; hexanes, acetone, CH_2Cl_2, and MeOH, simple distillation; chlorobenzene and MeCN, distilled by rotary evaporation and aspirated with N_2. The following were used as received: C_6D_6, toluene-d_8, $CDCl_3$, THF-d_8, CD_2Cl_2 (5 × deutero GmbH), Al_2O_3 (neutral, Macherey-Nagel), Grubbs catalyst (Aldrich), PtO_2, MeLi (1.6 M in Et_2O), Ph_2Zn, NH_4^+ I^-, n-Bu_4N^+ BF_4^-, Ph_3PO (6 × Acros), and NaI (Riedel). The following were synthesized by literature procedures: $Re(CO)_5(X)$ (X = Cl/Br),[15] ($P((CH_2)_nCH{=}CH_2)_3$)$_2$ (**1**; n = 6, **a**; 7, **b**; 8, **c**),[17] and $[Re_2(CO)_4(NO)_2(Cl)_2(\mu\text{-}Cl)_2]$.[22]

*mer,trans-Re(CO)$_3$(Cl)(P((CH$_2$)$_6$CH=CH$_2$)$_3$)$_2$ (**2a**).* A Schlenk flask was charged with $Re(CO)_5(Cl)$ (0.335 g, 0.926 mmol), chlorobenzene (20 mL), and **1a** (0.677 g, 1.86 mmol), and fitted with a condenser. The yellow solution was stirred for 21 h at 140 °C (oil bath temperature) and turned orange with gas evolution. The solvent was removed by rotary evaporation and oil pump vacuum. The residue was chromatographed (Al_2O_3 column, 3 × 15 cm, 4:1 v/v hexanes/CH_2Cl_2). The solvent was removed from the product containing fractions by oil pump vacuum to give **2a** (0.839 g, 0.811 mmol, 88%) as a viscous yellow oil. Anal. Calcd (%) for $C_{51}H_{90}ClO_3P_2Re$: C 59.19, H 8.77; found C 58.83, H 8.99.

NMR (δ/ppm): ^1H (C_6D_6, 400 MHz)[38] 5.77 (ddt, $^3J_{HHtrans}$ = 16.9 Hz, $^3J_{HHcis}$ = 10.2 Hz, $^3J_{HH}$ = 6.7 Hz, 6H, C*H*=), 5.04 (br d, $^3J_{HHtrans}$ = 17.1 Hz, 6H, =CH$_E$H$_Z$), 4.98 (br d, $^3J_{HHcis}$ = 10.2 Hz, 6H, =CH$_E$H$_Z$), 2.06−1.92 (br m, 24H, CH_2CH=CH$_2$/PCH_2), 1.68−1.56 (br m, 12H, PCH$_2$CH_2), 1.38−1.22 (br m, 36H, CH_2); $^{13}C\{^1H\}$ (toluene-d_8, 100 MHz)[38] 195.3 (t, $^2J_{CP}$ = 8.9 Hz, CO *trans* to CO), 191.8 (t, $^2J_{CP}$ = 6.5 Hz, CO *trans* to Cl), 139.1 (s, CH=), 114.6 (s, =CH$_2$), 34.1 (s, CH$_2$), 31.3 (virtual t,[21] $^3J_{CP}$ = 6.1 Hz, PCH$_2$CH$_2$CH$_2$), 29.2 (s, CH$_2$), 29.1 (s, CH$_2$), 27.4 (virtual t,[21] $^1J_{CP}$ = 14.3 Hz, PCH$_2$), 23.9 (s, PCH$_2$CH$_2$); $^{31}P\{^1H\}$ (C_6D_6, 162 MHz) −8.2 (s). **IR**: Table 1. **MS**:[39] 1035 ([**2a**]$^+$, 5%), 1007 ([**2a** − CO]$^+$, 100%), 1000 ([**2a** − Cl]$^+$, 90%), 979 ([**2a** − 2CO]$^+$, 6%).

*mer,trans-Re(CO)$_3$(Cl)(P((CH$_2$)$_7$CH=CH$_2$)$_3$)$_2$ (**2b**).* $Re(CO)_5(Cl)$ (0.500 g, 1.38 mmol), chlorobenzene (15 mL), and **1b** (1.125 g, 2.766 mmol) were combined in a procedure analogous to that used for **2a**. An identical workup gave **2b** (1.464 g, 1.308 mmol, 95%) as a viscous yellow oil. Anal. Calcd (%) for $C_{57}H_{102}ClO_3P_2Re$: C 61.18, H 9.19; found C 60.88, H 9.29.

NMR (C_6D_6, δ/ppm): ^1H (300 MHz)[40] 5.77 (ddt, $^3J_{HHtrans}$ = 16.8 Hz, $^3J_{HHcis}$ = 10.3 Hz, $^3J_{HH}$ = 6.6 Hz, 6H, C*H*=), 5.02 (br d, $^3J_{HHtrans}$ = 17.1 Hz, 6H, =CH$_E$H$_Z$), 4.97 (br d, $^3J_{HHcis}$ = 10.1 Hz, 6H, =CH$_E$H$_Z$), 2.15−1.88 (br m, 24H, CH_2CH=CH$_2$/PCH_2), 1.71−1.52 (br m, 12H, PCH$_2$CH_2), 1.42−1.12 (br m, 48H, CH_2); $^{13}C\{^1H\}$ (75 MHz)[40] 195.5 (t, $^2J_{CP}$ = 9.0 Hz, CO *trans* to CO), 192.0 (t, $^2J_{CP}$ = 6.1 Hz, CO *trans* to Cl), 139.1 (s, CH=), 114.5 (s, =CH$_2$), 34.1 (s, CH$_2$), 31.4 (virtual t,[21] $^3J_{CP}$ = 6.1 Hz, PCH$_2$CH$_2$CH$_2$), 29.4 (s, CH$_2$), 29.3 (s, CH$_2$), 29.2 (s, CH$_2$), 27.4 (virtual t,[21] $^1J_{CP}$ = 14.3 Hz, PCH$_2$), 23.9 (s, PCH$_2$CH$_2$); $^{31}P\{^1H\}$ (121 MHz) −8.2 (s). **IR**: Table 1. **MS**:[39] 1091 ([**2b** − CO]$^+$, 100%), 1084 ([**2b** − Cl]$^+$, 50%).

*mer,trans-Re(CO)$_3$(Cl)(P((CH$_2$)$_8$CH=CH$_2$)$_3$)$_2$ (**2c**).* $Re(CO)_5(Cl)$ (0.500 g, 1.38 mmol), chlorobenzene (15 mL), and **1c** (1.240 g, 2.763 mmol) were combined in a procedure analogous to that used for **2a**. An identical workup gave **2c** (1.154 g, 0.9599 mmol, 69%) as a viscous yellow oil. Anal. Calcd (%) for $C_{63}H_{114}ClO_3P_2Re$: C 62.89, H 9.55; found C 63.25, H 9.52.

NMR (C_6D_6, δ/ppm): ^1H (400 MHz)[40] 5.78 (ddt, $^3J_{HHtrans}$ = 16.9 Hz, $^3J_{HHcis}$ = 10.2 Hz, $^3J_{HH}$ = 6.7 Hz, 6H, C*H*=), 5.03 (br d, $^3J_{HHtrans}$ = 17.1 Hz, 6H, =CH$_E$H$_Z$), 4.98 (br d, $^3J_{HHcis}$ = 10.2 Hz, 6H, =CH$_E$H$_Z$), 2.09−2.02 (br m, 12H, CH_2CH=CH$_2$), 2.01−1.94 (br m, 12H, PCH_2), 1.72−1.59 (br m, 12H, PCH$_2$CH_2), 1.42−1.18 (br m, 60H, CH_2); $^{13}C\{^1H\}$ (100 MHz)[40] 195.5 (t, $^2J_{CP}$ = 8.4 Hz, CO *trans* to CO), 192.0 (t, $^2J_{CP}$ = 6.1 Hz, CO *trans* to Cl), 139.2 (s, CH=), 114.5 (s, =CH$_2$), 34.2 (s, CH$_2$), 31.4 (virtual t,[21] $^3J_{CP}$ = 6.1 Hz, PCH$_2$CH$_2$CH$_2$), 29.7 (s, CH$_2$), 29.6 (s, CH$_2$), 29.4 (s, CH$_2$), 29.3 (s, CH$_2$), 27.5 (virtual t,[21] $^1J_{CP}$ = 13.7 Hz, PCH$_2$), 24.0 (s, PCH$_2$CH$_2$); $^{31}P\{^1H\}$ (162 MHz) −8.2 (s). **IR**: Table 1. **MS**:[39] 1203 ([**2c**]$^+$, 10%), 1175 ([**2c** − CO]$^+$, 60%), 1168 ([**2c** − Cl]$^+$, 100%).

*mer,trans-Re(CO)$_3$(Br)(P((CH$_2$)$_6$CH=CH$_2$)$_3$)$_2$ (**3a**).* $Re(CO)_5(Br)$ (0.500 g, 1.23 mmol), chlorobenzene (20 mL), and **1a** (0.900 g, 2.47 mmol) were combined in a procedure analogous to that used for **2a**. An identical workup gave **3a** (0.975 g, 0.903 mmol, 73%) as a viscous yellow oil. Anal. Calcd (%) for $C_{51}H_{90}BrO_3P_2Re$: C 56.75, H 8.40; found C 56.81, H 7.95.

NMR (C_6D_6, δ/ppm): ^1H (300 MHz)[40] 5.77 (ddt, $^3J_{HHtrans}$ = 16.9 Hz, $^3J_{HHcis}$ = 10.2 Hz, $^3J_{HH}$ = 6.7 Hz, 6H, C*H*=), 5.04 (br d, $^3J_{HHtrans}$ = 17.1 Hz, 6H, =CH$_E$H$_Z$), 4.99 (br d, $^3J_{HHcis}$ = 10.3 Hz, 6H, =CH$_E$H$_Z$), 2.11−2.00 (br m, 12H, CH_2CH=CH$_2$), 1.99−1.91 (br m, 12H, PCH_2), 1.69−1.51 (br m, 12H, PCH$_2$CH_2), 1.49−1.20 (br m, 36H, CH_2); $^{13}C\{^1H\}$ (75 MHz)[40] 194.6 (t, $^2J_{CP}$ = 8.9 Hz, CO *trans* to CO), 191.5 (t, $^2J_{CP}$ = 6.4 Hz, CO *trans* to Br), 139.1 (s, CH=), 114.6 (s, =CH$_2$), 34.1 (s, CH$_2$), 31.2 (virtual t,[21] $^3J_{CP}$ = 6.6 Hz, PCH$_2$CH$_2$CH$_2$), 29.1 (s, CH$_2$), 29.0 (s, CH$_2$), 27.9 (virtual t,[21] $^1J_{CP}$ = 14.4 Hz, PCH$_2$), 24.0 (s, PCH$_2$CH$_2$); $^{31}P\{^1H\}$ (121 MHz) −13.2 (s). **IR**: Table 1. **MS**:[39] 1079 ([**3a**]$^+$, 5%), 1051 ([**3a** − CO]$^+$, 100%), 1022[41] ([**3a** − 2CO]$^+$, 5%), 1000 ([**3a** − Br]$^+$, 95%).

*mer,trans-Re(CO)$_3$(Br)(P((CH$_2$)$_7$CH=CH$_2$)$_3$)$_2$ (**3b**).* $Re(CO)_5(Br)$ (0.503 g, 1.24 mmol), chlorobenzene (10 mL), and **1b** (1.008 g, 2.478 mmol) were combined in a procedure analogous to that used for **2a**. A similar workup (Al_2O_3 column, 3 × 20 cm, 4:1 v/v hexanes/CH_2Cl_2) gave **3b** (0.769 g, 0.661 mmol, 53%) as a viscous yellow oil. Anal. Calcd (%) for $C_{57}H_{102}BrO_3P_2Re$: C 58.84, H 8.84; found C 61.82, H 9.58.[42]

NMR (C_6D_6, δ/ppm): ^1H (300 MHz)[40] 5.78 (ddt, $^3J_{HHtrans}$ = 16.9 Hz, $^3J_{HHcis}$ = 10.2 Hz, $^3J_{HH}$ = 6.7 Hz, 6H, C*H*=), 5.03 (br d, $^3J_{HHtrans}$ = 17.1 Hz, 6H, =CH$_E$H$_Z$), 4.99 (br d, $^3J_{HHcis}$ = 10.7 Hz, 6H, =CH$_E$H$_Z$), 2.13−2.03 (br m, 12H, CH_2CH=CH$_2$), 2.02−1.92 (br m, 12H, PCH_2), 1.71−1.56 (br m, 12H, PCH$_2$CH_2), 1.39−1.17 (br m, 48H, CH_2); $^{13}C\{^1H\}$ (100 MHz)[40] 194.6 (t, $^2J_{CP}$ = 9.1 Hz, CO *trans* to CO), 191.5 (t, $^2J_{CP}$ = 6.5 Hz, CO *trans* to Br), 139.1 (s, CH=), 114.5 (s, =CH$_2$), 34.1 (s, CH$_2$), 31.3 (virtual t,[21] $^3J_{CP}$ = 6.1 Hz, PCH$_2$CH$_2$CH$_2$), 29.4 (s, CH$_2$), 29.3 (s, CH$_2$), 29.2 (s, CH$_2$), 28.0 (virtual t,[21] $^1J_{CP}$ = 14.3 Hz, PCH$_2$), 24.0 (s, PCH$_2$CH$_2$); $^{31}P\{^1H\}$ (121 MHz) −13.2 (s). **IR**: Table 1. **MS**:[43] 1164 ([**3b**]$^+$, 20%), 1135 ([**3b** − CO]$^+$, 100%), 1107 ([**3b** − 2CO]$^+$, 15%), 1084 ([**3b** − Br]$^+$, 75%).

DOI: 10.1021/acs.inorgchem.7b00909
Inorg. Chem. 2017, 56, 7454−7469

*mer,trans-Re(CO)$_3$(Br)(P((CH$_2$)$_8$CH=CH$_2$)$_3$)$_2$ (**3c**).* Re(CO)$_5$(Br) (0.420 g, 1.03 mmol), chlorobenzene (15 mL), and **1c** (0.927 g, 2.07 mmol) were combined in a procedure analogous to that used for **2a**. A similar workup (Al$_2$O$_3$ column, 3 × 20 cm, 4:1 v/v hexanes/CH$_2$Cl$_2$) gave **3c** (0.993 g, 0.796 mmol, 77%) as a viscous yellow oil. Anal. Calcd (%) for $C_{63}H_{114}BrO_3P_2Re$: C 60.65, H 9.21; found C 60.91, H 9.20.

NMR (C$_6$D$_6$, δ/ppm): **^{1}H** (300 MHz)[40] 5.80 (ddt, $^3J_{HHtrans}$ = 16.9 Hz, $^3J_{HHcis}$ = 10.1 Hz, $^3J_{HH}$ = 6.8 Hz, 6H, C*H*=), 5.05 (br d, $^3J_{HHtrans}$ = 17.3 Hz, 6H, =CH$_E$*H*$_Z$), 5.00 (br d, $^3J_{HHcis}$ = 10.3 Hz, 6H, =C*H*$_E$H$_Z$), 2.16−2.05 (br m, 12H, C*H*$_2$CH=CH$_2$), 2.05−1.93 (br m, 12H, PC*H*$_2$), 1.75−1.58 (br m, 12H, PCH$_2$C*H*$_2$), 1.44−1.17 (br m, 60H, C*H*$_2$); **^{13}C{^{1}H}** (100 MHz)[40] 194.7 (t, $^2J_{CP}$ = 9.0 Hz, *CO trans* to CO), 191.6 (t, $^2J_{CP}$ = 6.5 Hz, *CO trans* to Br), 139.2 (s, *C*H=), 114.5 (s, =CH$_2$), 34.2 (s, CH$_2$), 31.4 (virtual t,[21] $^3J_{CP}$ = 6.2 Hz, PCH$_2$CH$_2$CH$_2$), 29.7 (s, *C*H$_2$), 29.6 (s, CH$_2$), 29.4 (s, CH$_2$), 29.3 (s, CH$_2$), 28.0 (virtual t,[21] $^1J_{CP}$ = 14.5 Hz, PCH$_2$), 24.1 (s, PCH$_2$CH$_2$); **^{31}P{^{1}H}** (121 MHz) −13.2 (s). **IR**: Table 1. **MS**:[43] 1247 ([**3c**]$^+$, 20%), 1219 ([**3c** − CO]$^+$, 100%), 1192 ([**3c** − 2CO]$^+$, 20%), 1168 ([**3c** − Br]$^+$, 35%).

*cis,trans-Re(CO)(NO)(Cl)$_2$(P((CH$_2$)$_6$CH=CH$_2$)$_3$)$_2$ (**4a**).*[23] [Re$_2$(CO)$_4$(NO)$_2$(Cl)$_2$(μ-Cl)$_2$] (0.200 g, 0.291 mmol), MeCN (30 mL), and **1a** (0.584 g, 1.60 mmol) were combined in a procedure analogous to that used for **2a** (3 h at 120 °C oil bath temperature). A similar workup (Al$_2$O$_3$ column, 3 × 15 cm, CH$_2$Cl$_2$) gave **4a** (0.348 g, 0.333 mmol, 57%) as a viscous yellow oil. Anal. Calcd (%) for $C_{49}H_{90}Cl_2NO_2P_2Re$: C 56.36, H 8.69; found C 56.71, H 8.92.

NMR (C$_6$D$_6$, δ/ppm): **^{1}H** (300 MHz)[40] 5.77 (ddt, 6H, $^3J_{HHtrans}$ = 16.9 Hz, $^3J_{HHcis}$ = 10.2 Hz, $^3J_{HH}$ = 6.7 Hz, C*H*=), 5.04 (br d, $^3J_{HHtrans}$ = 17.1 Hz, 6H, =CH$_E$*H*$_Z$), 4.98 (br d, $^3J_{HHcis}$ = 10.2 Hz, 6H, =C*H*$_E$H$_Z$), 2.31−2.10 (br m, 12H, C*H*$_2$CH=CH$_2$), 2.09−1.89 (br m, 12H, PC*H*$_2$), 1.80−1.55 (br m, 2H, PCH$_2$C*H*$_2$), 1.48−1.12 (br m, 36H, C*H*$_2$); **^{13}C{^{1}H}** (75 MHz)[40] 204.2 (t, $^2J_{CP}$ = 7.0 Hz, *CO*), 139.0 (s, *C*H=), 114.5 (s, =CH$_2$), 34.0 (s, CH$_2$), 31.3 (virtual t,[21] $^3J_{CP}$ = 6.2 Hz, PCH$_2$CH$_2$CH$_2$), 29.0 (s, CH$_2$), 28.9 (s, CH$_2$), 23.4 (s, PCH$_2$CH$_2$), 23.3 (virtual t,[21] $^1J_{CP}$ = 14.3 Hz, PCH$_2$); **^{31}P{^{1}H}** (121 MHz) −8.3 (s). **IR**: Table 1. **MS**:[39] 1043[41] ([**4a**]$^+$, 1%), 1015[41] ([**4a** − CO]$^+$, 100%), 980[41] ([**4a** − Cl − CO]$^+$, 50%).

*Alkene Metathesis of **2a**.* A three-necked flask was charged with **2a** (0.550 g, 0.531 mmol) and chlorobenzene (500 mL; the resulting solution is ca. 0.0011 M in **2a**), and fitted with a condenser. Grubbs' catalyst (0.027 g, 0.033 mmol, 6 mol %) was added. The mixture was stirred for 2 d, while N$_2$ was bubbled through the solution to remove the ethene. The solution was filtered through Al$_2$O$_3$, which was rinsed with CH$_2$Cl$_2$. The solvent was removed from the combined filtrates by oil pump vacuum to give **5*a** (0.383 g, 0.403 mmol, 76%)[44] as a viscous yellow oil.

NMR (C$_6$D$_6$, δ/ppm): **^{1}H** (300 MHz) 5.60−5.42 (br m, 6H, C*H*=), 2.22−1.98 (br m, 12H, C*H*$_2$CH=CH), 1.90−1.62 (br m, 12H, PC*H*$_2$), 1.60−1.18 (br m, 48H, C*H*$_2$); **^{31}P{^{1}H}** (121 MHz) −1.8 (s, 45% of integral), −3.2 (s, 13%), −4.6 (s, 14%), −6.4 (s, 28%). **MS**:[39] 950 ([**M**]$^+$, 7%), 922 ([**M** − CO]$^+$, 100%), 915 ([**M** − Cl]$^+$, 35%).

*mer,trans-Re(CO)$_3$(Cl)(P((CH$_2$)$_{14}$)$_3$P) (**7a**) and mer,trans-Re(CO)$_3$(Cl)(P(CH$_2$)$_{13}$CH$_2$)((CH$_2$)$_{14}$)(P(CH$_2$)$_{13}$CH$_2$) (**7′a**).* A Fischer−Porter bottle was charged with **5*a** (0.383 g, 0.403 mmol; the entire quantity prepared above), THF (15 mL), and PtO$_2$ (0.010 g, 0.044 mmol), connected to a H$_2$ cylinder, and partially evacuated. Then H$_2$ was introduced (5 bar), and the suspension was stirred. After 5 d, the solvent was removed by oil pump vacuum. The residue was chromatographed (Al$_2$O$_3$ column, 3 × 25 cm, 4:1 v/v hexanes/CH$_2$Cl$_2$). The solvent was removed from the product containing fractions by rotary evaporation and oil pump vacuum to give **7a** (0.311 g, 0.325 mmol, 81%; 61% from **2a**) as a white solid and **7′a** (0.030 g, 0.031 mmol, 8%; 6% from **2a**) as an iridescent white powder.

7a: mp 230 °C, dec (gradual darkening, >180 °C). **DSC/TGA**: Table s1. Anal. Calcd (%) for $C_{45}H_{84}ClO_3P_2Re$: C 56.49, H 8.85; found C 56.67, H 8.92.

NMR (C$_6$D$_6$, δ/ppm): **^{1}H** (300 MHz)[38] 1.95−1.81 (br m, 12H, PC*H*$_2$), 1.75−1.60 (br m, 12H, PCH$_2$C*H*$_2$), 1.52−1.25 (br m, 60H, C*H*$_2$); **^{13}C{^{1}H}** (75 MHz):[38] 195.3 (t, $^2J_{CP}$ = 9.0 Hz, *CO trans* to CO), 191.9 (t, $^2J_{CP}$ = 6.3 Hz, *CO trans* to Cl), 30.4 (virtual t,[21] $^3J_{CP}$ = 6.3 Hz, PCH$_2$CH$_2$CH$_2$), 29.2 (virtual t,[21] $^1J_{CP}$ = 14.4 Hz, PCH$_2$), 28.6 (s, CH$_2$), 28.4 (s, CH$_2$), 28.0 (s, CH$_2$), 27.8 (s, CH$_2$), 23.6 (s, PCH$_2$CH$_2$); **^{31}P{^{1}H}** (121 MHz): −5.5 (s). **IR**: Table 1. **MS**:[39] 956[41] ([**7a**]$^+$, 13%), 928[41] ([**7a** − CO]$^+$, 100%), 921[41] ([**7a** − Cl]$^+$, 67%).

7′a: mp 70 °C.

NMR (C$_6$D$_6$, δ/ppm): **^{1}H** (300 MHz)[40] 2.23−1.63 (br m, 24H, PC*H*$_2$/PCH$_2$C*H*$_2$), 1.62−1.12 (br m, 60H, C*H*$_2$); **^{13}C{^{1}H}** (100 MHz)[40] 195.5 (t, $^2J_{CP}$ = 9.2 Hz, *CO trans* to CO), 192.0 (t, $^2J_{CP}$ = 6.0 Hz, *CO trans* to Cl), 30.7 (virtual t,[21] $^3J_{CP}$ = 6.5 Hz, PCH$_2$CH$_2$CH$_2$), 28.9 (virtual t,[21] $^3J_{CP}$ = 5.5 Hz, PC′H$_2$C′H$_2$C′H$_2$), 28.6 (s, CH$_2$), 28.4 (s, CH$_2$),[45] 28.2 (virtual t,[21] $^1J_{CP}$ = 14.8 Hz, PCH$_2$),[45] 27.8 (s, CH$_2$), 27.7 (s, CH$_2$), 27.2 (s, C′H$_2$), 27.1 (s, C′H$_2$), 26.8 (s, C′H$_2$),[45] 26.7 (virtual t,[21] $^1J_{CP}$ = 13.8 Hz, PC′H$_2$),[45] 26.5 (s, C′H$_2$), 23.8 (s, PCH$_2$CH$_2$), 22.2 (s, PC′H$_2$C′H$_2$); **^{31}P{^{1}H}** (121 MHz) −7.2 (s). **IR**: Table 1.

*Alkene Metathesis of **2b**.* Complex **2b** (0.450 g, 0.404 mmol), chlorobenzene (350 mL; the resulting solution is ca. 0.0011 M in **2b**), and Grubbs' catalyst (0.033 g, 0.040 mmol, 10 mol %) were combined in a procedure analogous to that used for **2a**. An identical workup gave **5*b** (0.412 g, 0.398 mmol, 99%)[44] as a viscous yellow oil.

NMR (C$_6$D$_6$, δ/ppm): **^{1}H** (300 MHz) 5.65−5.20 (m, 6H, C*H*=), 2.27−1.58 (m, 36H, C*H*$_2$CH=CH/PC*H*$_2$), 1.52−1.03 (m, 48H, C*H*$_2$); **^{31}P{^{1}H}** (121 MHz) −7.0 (s, 6% of integral), −7.2 (s, 7%), −7.5 (s, 41%), −7.7 (m, 47%). **MS**:[39] 1036[41] ([**M**]$^+$, 30%), 1006[41] ([**M** − CO]$^+$, 100%), 1000 ([**M** − Cl]$^+$, 80%).

*mer,trans-Re(CO)$_3$(Cl)(P(CH$_2$)$_{15}$CH$_2$)((CH$_2$)$_{16}$)(P(CH$_2$)$_{15}$CH$_2$) (**7′b**).*[46,47] Complex **5*b** (0.412 g, 0.398 mmol; the entire quantity prepared above), THF (20 mL), and PtO$_2$ (0.009 g, 0.04 mmol) were combined in a procedure analogous to that used for **7a**. An identical workup (Al$_2$O$_3$ column, 3 × 25 cm, 4:1 v/v hexanes/CH$_2$Cl$_2$) gave **7′b** (0.114 g, 0.110 mmol, 28%; 27% from **2b**) as a sticky yellow oil. Anal. Calcd (%) for $C_{51}H_{96}ClO_3P_2Re$: C 58.85, H 9.30; found C 58.90, H 9.25.

NMR (C$_6$D$_6$, δ/ppm): **^{1}H** (300 MHz)[40] 2.16−1.82 (br m, 12H, PC*H*$_2$), 1.81−1.55 (br m, 12H, PCH$_2$C*H*$_2$), 1.53−1.14 (br m, 72H, C*H*$_2$); **^{13}C{^{1}H}** (100 MHz):[40] 195.5 (t, $^2J_{CP}$ = 9.0 Hz, *CO trans* to CO), 191.9 (t, $^2J_{CP}$ = 6.1 Hz, *CO trans* to Cl), 30.9 (virtual t,[21] $^3J_{CP}$ = 6.6 Hz, PCH$_2$CH$_2$CH$_2$), 30.1 (virtual t,[21] $^3J_{CP}$ = 5.7 Hz, PC′H$_2$C′H$_2$C′H$_2$), 28.81 (s, CH$_2$), 28.78 (s, CH$_2$), 28.5 (s, CH$_2$), 28.2 (s, C′H$_2$),[45] 28.15 (virtual t,[21] $^1J_{CP}$ = 14.5 Hz, PCH$_2$),[45] 28.14 (s, CH$_2$),[45] 27.84 (s, C′H$_2$), 27.78 (s, C′H$_2$), 27.4 (s, C′H$_2$), 26.6 (virtual t,[21] $^1J_{CP}$ = 14.0 Hz, PC′H$_2$), 23.9 (s, PCH$_2$CH$_2$), 23.0 (s, PC′H$_2$C′H$_2$); **^{31}P{^{1}H}** (121 MHz) −7.5 (s). **IR**: Table 1. **MS**:[39] 1041 ([**7′b**]$^+$, 10%), 1013 ([**7′b** − CO]$^+$, 100%), 1006 ([**7′b** − Cl]$^+$, 68%).

*Alkene Metathesis of **2c**.* Complex **2c** (0.546 g, 0.454 mmol), chlorobenzene (400 mL; the resulting solution is ca. 0.0011 M in **2c**), and Grubbs catalyst (0.019 g, 0.023 mmol, 5 mol %) were combined in a procedure analogous to that used for **2a**. An identical workup gave **5*c** (0.487 g, 0.435 mmol, 96%)[44] as a viscous yellow oil.

NMR (C$_6$D$_6$, δ/ppm): **^{1}H** (300 MHz) 5.55−5.35 (br m, 6H, C*H*=), 2.18−2.00 (br m, 12H, C*H*$_2$CH=CH), 1.99−1.78 (br m, 12H, PC*H*$_2$), 1.77−1.55 (br m, 12H, PCH$_2$C*H*$_2$), 1.54−1.18 (br m, 60H, C*H*$_2$); **^{31}P{^{1}H}** (121 MHz) −5.3 (s, 35% of integral), −5.7 (s, 14%), −6.1 (s, 10%), −6.9 (s, 41%). **MS**:[39] 1119 ([**M**]$^+$, 20%), 1091 ([**M** − CO]$^+$, 70%), 1084 ([**M** − Cl]$^+$, 100%).

*mer,trans-Re(CO)$_3$(Cl)(P((CH$_2$)$_{18}$)$_3$P) (**7c**) and mer,trans-Re(CO)$_3$(Cl)(P(CH$_2$)$_{17}$CH$_2$)((CH$_2$)$_{18}$)(P(CH$_2$)$_{17}$CH$_2$) (**7′c**).*[46] Complex **5*c** (0.487 g, 0.435 mmol; the entire quantity prepared above), THF (10 mL), and PtO$_2$ (0.010 g, 0.044 mmol) were combined in a procedure analogous to that used for **7a** and **7′a**. An identical workup gave **7c** (0.126 g, 0.112 mmol, 26%; 25% from **2c**) and **7′c** (0.057 g, 0.051 mmol, 12%; 11% from **2c**) as sticky pale yellow oils.

7c: Anal. Calcd (%) for $C_{57}H_{108}ClO_3P_2Re$: C 60.85, H 9.68; found C 61.22, H 9.96.

NMR (C$_6$D$_6$, δ/ppm): **^{1}H** (300 MHz)[40] 2.09−1.89 (br m, 12H, PC*H*$_2$), 1.72−1.55 (br m, 12H, PCH$_2$C*H*$_2$), 1.54−1.25 (br m, 84H, C*H*$_2$); **^{13}C{^{1}H}** (100 MHz)[40] 195.4 (t, $^2J_{CP}$ = 8.8 Hz, *CO trans* to CO), 191.8 (t, $^2J_{CP}$ = 6.5 Hz, *CO trans* to Cl), 30.7 (virtual t,[21] $^3J_{CP}$ = 6.0 Hz,

DOI: 10.1021/acs.inorgchem.7b00909
Inorg. Chem. 2017, 56, 7454−7469

$PCH_2CH_2CH_2$), 29.1 (s, CH_2), 28.9 (s, CH_2), 28.69 (s, CH_2), 28.65 (s, CH_2), 28.56 (s, CH_2), 28.4 (s, CH_2), 27.4 (virtual t, $^{21}J_{CP}$ = 14.3 Hz, PCH_2), 23.5 (s, PCH_2CH_2); $^{31}P\{^1H\}$ (121 MHz) −7.3 (s). **IR**: Table 1. **MS**:[39] 1097 ([**7c** − CO]$^+$, 100%).

7′c: **NMR** (C_6D_6, δ/ppm): ^1H (300 MHz)[40] 2.20−1.88 (br m, 12H, PCH_2), 1.87−1.60 (br m, 12H, PCH_2CH_2), 1.59−1.17 (br m, 84H, CH_2). $^{13}C\{^1H\}$ (100 MHz)[40] 195.5 (t, $^2J_{CP}$ = 9.2 Hz, *CO trans* to CO), 192.0 (t, $^2J_{CP}$ = 6.0 Hz, *CO trans* to Cl), 31.0 (virtual t, $^{21}\,^3J_{CP}$ = 6.5 Hz, $PCH_2CH_2CH_2$), 30.8 (virtual t, $^{21}\,^3J_{CP}$ = 5.5 Hz, $PC'H_2C'H_2C'H_2$), 28.91 (s, CH_2), 28.86 (s, CH_2 or $C'H_2$), 28.75 (s, CH_2 or $C'H_2$), 28.69 (s, CH_2 or $C'H_2$), 28.63 (s, CH_2 or $C'H_2$), 28.62 (s, CH_2 or $C'H_2$), 28.4 (s, $C'H_2$), 28.3 (s, $C'H_2$), 28.2 (virtual t, $^{21}\,^1J_{CP}$ = 14.8 Hz, PCH_2), 28.0 (s, $C'H_2$), 27.5 (s, $C'H_2$), 26.7 (virtual t, $^{21}\,^1J_{CP}$ = 13.8 Hz, $PC'H_2$), 24.0 (s, PCH_2CH_2), 23.3 (s, $PC'H_2C'H_2$); $^{31}P\{^1H\}$ (121 MHz) −7.7 (s). **IR**: Table 1. **MS**:[43] 1128 ([**7′c**]$^+$, 50%), 852 ([P((CH_2)$_{18}$)P + 2O]$^+$, 55%), 836 ([P((CH_2)$_{18}$)P + O]$^+$, 50%), 820 ([P((CH_2)$_{18}$)P]$^+$, 10%).

Alkene Metathesis of ***3a***. Complex **3a** (0.640 g, 0.593 mmol), chlorobenzene (500 mL; the resulting solution is ca. 0.0012 M in **3a**), and Grubbs catalyst (0.027 g, 0.033 mmol, 6 mol %) were combined in a procedure analogous to that used for **2a**. An identical workup gave **6*a** (0.531 g, 0.534 mmol, 90%)[44] as a viscous yellow oil.

NMR (δ/ppm): ^1H (C_6D_6, 300 MHz) 5.58−5.20 (br m, 6H, C*H*═), 2.27−1.92 (br m, 12H, CH_2CH═CH), 1.91−1.65 (br m, 12H, PCH_2), 1.62−1.15 (br m, 48H, CH_2); $^{31}P\{^1H\}$ ($CDCl_3$, 162 MHz): −6.0 (s, 41% of integral), −7.7 (s, 11%), −8.9 (s, 14%), −11.4 (s, 33%). **MS**:[39] 994 ([**M**]$^+$, 14%), 966 ([**M** − CO]$^+$, 100%), 913 (overlapping ions: [**M** − 3CO]$^+$ (911), [**M** − Br]$^+$ (915), 34%).

mer,trans-Re(CO)$_3$(Br)(P((CH$_2$)$_{14}$)$_3$P) ***(8a)***. Complex **6*a** (0.531 g, 0.534 mmol; the entire quantity prepared above), THF (15 mL), and PtO_2 (0.020 g, 0.088 mmol) were combined in a procedure analogous to that used for **7a**. An identical workup gave **8a** (0.220 g, 0.220 mmol, 41%; 37% from **3a**) as a white solid, mp 254 °C, dec (gradual darkening, >180 °C). **DSC**/**TGA**: Table s1. Anal. Calcd (%) for $C_{45}H_{84}BrO_3P_2Re$: C 53.98, H 8.46; found C 53.70, H 8.33.

NMR (C_6D_6, δ/ppm): ^1H (300 MHz)[40] 2.00−1.82 (br m, 12H, PCH_2), 1.78−1.59 (br m, 12H, PCH_2CH_2), 1.55−1.28 (br m, 60H, CH_2); $^{13}C\{^1H\}$ (100 MHz)[40] 194.6 (t, $^2J_{CP}$ = 8.6 Hz, *CO trans* to CO), 191.3 (t, $^2J_{CP}$ = 6.3 Hz, *CO trans* to Br), 30.3 (virtual t, $^{21}\,^3J_{CP}$ = 6.5 Hz, $PCH_2CH_2CH_2$), 29.9 (virtual t, $^{21}\,^1J_{CP}$ = 14.8 Hz, PCH_2), 28.6 (s, CH_2), 28.5 (s, CH_2), 28.0 (s, CH_2), 27.9 (s, CH_2), 23.8 (s, PCH_2CH_2); $^{31}P\{^1H\}$ (121 MHz): −10.3 (s). **IR**: Table 1. **MS**:[39] 1000 ([**8a**]$^+$, 28%), 972 ([**8a** − CO]$^+$, 100%), 919 (overlapping ions: [**8a** − 3CO]$^+$ (917) and [**8a** − Br]$^+$ (921), 42%).

Alkene Metathesis of ***3b***. Complex **3b** (0.750 g, 0.644 mmol), chlorobenzene (600 mL; the resulting solution is ca. 0.0011 M in **3b**), and Grubbs catalyst (0.027 g, 0.032 mmol, 5 mol %) were combined in a procedure analogous to that used for **2a**. An identical workup gave **6*b** (0.624 g, 0.578 mmol, 90%)[44] as a viscous yellow oil.

NMR (C_6D_6, δ/ppm): ^1H (400 MHz) 5.63−5.24 (br m, 6H, C*H*═), 2.25−1.55 (br m, 36H, CH_2CH═CH/PCH_2/PCH_2CH_2), 1.53−1.05 (br m, 48H, CH_2); $^{31}P\{^1H\}$ (162 MHz): −12.0 (s, 4% of integral), −12.2 (s, 4%), −12.4 (d, 28%), −12.6 (d, 25%), −12.9 (m, 38%). **MS**:[43] 1052 ([**M** − CO]$^+$, 30%), 1000 ([**M** − Br]$^+$, 50%), 762 ([P((CH_2)$_7$CH═CH(CH_2)$_7$)P + 2O]$^+$, 100%).

mer,trans-Re(CO)$_3$(Br)(P(CH$_2$)$_{15}$CH$_2$)((CH$_2$)$_{16}$)(P(CH$_2$)$_{15}$CH$_2$) ***(8′b)***.[46] Complex **6*b** (0.624 g, 0.578 mmol; the entire quantity prepared above), THF (10 mL), and PtO_2 (0.013 g, 0.059 mmol) were combined in a procedure analogous to that used for **7a**. An identical workup gave **8′b** (0.143 g, 0.132 mmol, 23%; 20% from **3b**) as a sticky white oil. Anal. Calcd (%) for $C_{51}H_{96}BrO_3P_2Re$: C 56.44, H 8.92; found C 56.70, H 9.21.

NMR (C_6D_6, δ/ppm): ^1H (300 MHz)[40] 2.22−1.89 (br m, 12H, PCH_2), 1.85−1.58 (br m, 12H, PCH_2CH_2), 1.55−1.17 (br m, 72H, CH_2); $^{13}C\{^1H\}$ (75 MHz)[40] 194.7 (t, $^2J_{CP}$ = 8.7 Hz, *CO trans* to CO), 191.5 (t, $^2J_{CP}$ = 7.2 Hz, *CO trans* to Br), 30.8 (virtual t, $^{21}\,^3J_{CP}$ = 6.7 Hz, $PCH_2CH_2CH_2$), 30.0 (virtual t, $^{21}\,^3J_{CP}$ = 5.8 Hz, $PC'H_2C'H_2C'H_2$), 28.8 (s, CH_2), 28.51 (s, CH_2), 28.48 (s, CH_2), 28.21 (s, $C'H_2$), 28.18 (s, CH_2), 27.82 (s, $C'H_2$), 27.76 (s, $C'H_2$), 27.4 (s, $C'H_2$), 27.2 (virtual t, $^{21}\,^1J_{CP}$ = 13.7 Hz, $PC'H_2$),[48] 24.0 (s, PCH_2CH_2), 23.1 (s, $PC'H_2C'H_2$), $^{31}P\{^1H\}$ (121 MHz) −12.6 (s). **IR**: Table 1. **MS**:[43] 1086 ([**8′b**]$^+$, 20%), 1057 ([**8′b** − CO]$^+$, 90%), 1006 ([**8′b** − Br]$^+$, 100%).

Alkene Metathesis of ***3c***. Complex **3c** (0.905 g, 0.725 mmol), chlorobenzene (700 mL; the resulting solution is ca. 0.0010 M in **3c**), and Grubbs catalyst (0.030 g, 0.036 mmol, 5 mol %) were combined in a procedure analogous to that used for **2a**. An identical workup gave **6*c** (0.701 g, 0.603 mmol, 83%)[44] as a viscous yellow oil.

NMR (C_6D_6, δ/ppm): ^1H (300 MHz) 5.61−5.30 (br m, 6H, C*H*═), 2.26−1.86 (br m, 24H, CH_2CH═CH/PCH_2), 1.79−1.10 (br m, 72H, CH_2); $^{31}P\{^1H\}$ (121 MHz): −10.2 (s, 26% of integral), −10.7 (s, 17%), −11.1 (s, 17%), −12.0 (s, 40%). **MS**:[39] 1162[41] ([**M**]$^+$, 20%), 1134[41] ([**M** − CO]$^+$, 100%), 1081 (overlapping ions: [**M** − 3CO]$^+$ (1079), [**M** − Br]$^+$ (1083), 60%).

mer,trans-Re(CO)$_3$(Br)(P((CH$_2$)$_{18}$)$_3$P) ***(8c)***.[46] Complex **6*c** (0.701 g, 0.603 mmol; the entire quantity prepared above), THF (10 mL), and PtO_2 (0.014 g, 0.062 mmol) were combined in a procedure analogous to that used for **7a**. An identical workup gave **8c** (0.150 g, 0.128 mmol, 21%; 18% from **3c**) as a viscous yellow oil. Anal. Calcd (%) for $C_{57}H_{108}BrO_3P_2Re$: C 58.44, H 9.46; found C 59.88, H 9.25.[42]

NMR (C_6D_6, δ/ppm): ^1H (300 MHz)[40] 2.08−1.89 (br m, 12H, PCH_2), 1.71−1.52 (br m, 12H, PCH_2CH_2), 1.50−1.29 (br m, 84H, CH_2); $^{13}C\{^1H\}$ (100 MHz)[40] 194.6 (t, $^2J_{CP}$ = 8.9 Hz, *CO trans* to CO), 191.3 (t, $^2J_{CP}$ = 6.0 Hz, *CO trans* to Br), 30.5 (virtual t, $^{21}\,^3J_{CP}$ = 6.2 Hz, $PCH_2CH_2CH_2$), 29.1 (s, CH_2), 28.9 (s, CH_2), 28.8 (s, CH_2), 28.6 (s, CH_2), 28.3 (s, CH_2), 27.8 (s, CH_2), 27.9 (virtual t, $^{21}\,^1J_{CP}$ = 14.5 Hz, PCH_2), 23.5 (s, PCH_2CH_2); $^{31}P\{^1H\}$ (121 MHz) −12.6 (s). **IR**: Table 1. **MS**:[39] 1169 ([**8c**]$^+$, 35%), 1141 ([**8c** − CO]$^+$, 100%), 1090 ([**8c** − Br]$^+$, 100%).

Alkene Metathesis of ***4a***. Complex **4a** (0.296 g, 0.283 mmol), chlorobenzene (230 mL; the resulting solution is ca. 0.0012 M in **4a**), and Grubbs catalyst (0.011 g, 0.013 mmol, 5 mol %) were combined in a procedure analogous to that used for **2a**. An identical workup gave a viscous yellow oil (0.232 g, 0.242 mmol, 86%).[44]

NMR (C_6D_6, δ/ppm): ^1H (300 MHz) 5.65−5.18 (br m, 6H, C*H*═), 2.39−1.81 (br m, 24H, CH_2CH═CH/PCH_2), 1.68−1.09 (br m, 60H, CH_2); $^{31}P\{^1H\}$ (121 MHz): −4.7 (s, 34% of integral), −5.8 (s, 13%), −6.3 (s, 23%), −7.1 (s, 29%). **MS**:[39] 959 ([**M**]$^+$, 5%), 931 ([**M** − CO]$^+$, 100%), 894 ([**M** − Cl − CO]$^+$, 65%).

cis,trans-Re(CO)(NO)(Cl)$_2$(P((CH$_2$)$_{14}$)$_3$P) ***(9a)***. The crude metathesis product of **4a** (0.232 g, 0.242 mmol; the entire quantity prepared above), THF (15 mL), and PtO_2 (0.009 g, 0.04 mmol) were combined in a procedure analogous to that used for **7a**. A similar workup (Al_2O_3 column, 3 × 20 cm, 2:1 v/v hexanes/CH_2Cl_2) gave **9a** (0.039 g, 0.040 mmol, 17%; 14% from **4a**) as a white solid, mp 278 °C, dec (gradual darkening, >265 °C). **DSC**/**TGA**: Table s1. Anal. Calcd (%) for $C_{43}H_{84}Cl_2NO_2P_2Re$: C 53.45, H 8.76, N 1.45; found C 53.43, H 8.52, N 1.47.

NMR (C_6D_6, δ/ppm): ^1H (300 MHz)[40] 2.10−1.84 (br m, 12H, PCH_2), 1.80−1.60 (br m, 12H, PCH_2CH_2), 1.59−1.20 (m, 60H, CH_2); $^{13}C\{^1H\}$ (100 MHz)[40] 203.1 (t, $^2J_{CP}$ = 5.5 Hz, CO), 29.9 (virtual t, $^{21}\,^3J_{CP}$ = 6.5 Hz, $PCH_2CH_2CH_2$), 28.2 (s, CH_2), 28.1 (s, CH_2), 27.4 (s, CH_2), 27.3 (s, CH_2), 24.7 (virtual t, $^{21}\,^1J_{CP}$ = 14.2 Hz, PCH_2), 22.4 (s, PCH_2CH_2); $^{31}P\{^1H\}$ (121 MHz) − 7.1 (s). **IR**: Table 1. **MS**:[39] 967[41] ([**9a**]$^+$, 25%), 937[41] ([**9a** − CO]$^+$, 70%), 900[41] ([**9a** − NO − Cl]$^+$, 65%).

mer,trans-Re(CO)$_3$(I)(P((CH$_2$)$_6$CH═CH$_2$)$_3$)$_2$ ***(10a)***. A Schlenk flask was charged with **2a** (0.250 g, 0.242 mmol), NaI (0.181 g, 1.21 mmol), THF (20 mL), and acetone (10 mL). The yellow solution refluxed for 20 h. The solvent was removed by rotary evaporation and oil pump vacuum, and the residue was chromatographed (Al_2O_3 column, 1.5 × 15 cm, 4:1 v/v hexanes/CH_2Cl_2). The solvent was removed from the product containing fractions by oil pump vacuum to give **5a** (0.185 g, 0.164 mmol, 68%) as a viscous yellow oil. Anal. Calcd (%) for $C_{51}H_{90}IO_3P_2Re$: C 54.38, H 8.05; found C 54.34, H 7.80.

NMR (C_6D_6, δ/ppm): ^1H (300 MHz)[40] 5.77 (ddt, $^3J_{HHtrans}$ = 16.9 Hz, $^3J_{HHcis}$ = 10.2 Hz, $^3J_{HH}$ = 6.7 Hz, 6H, C*H*═), 5.04 (br d, $^3J_{HHtrans}$ = 17.2 Hz, 6H, ═CH_EH_Z), 4.99 (br d, $^3J_{HHcis}$ = 10.1 Hz, 6H, ═CH_EH_Z), 2.17−2.03 (br m, 12H, CH_2CH═CH_2), 2.02−1.91 (br m, 12H, PCH_2), 1.68−1.52 (br m, 12H, PCH_2CH_2), 1.39−1.21 (br m, 36H, CH_2);

DOI: 10.1021/acs.inorgchem.7b00909
Inorg. Chem. 2017, 56, 7454−7469

$^{13}C\{^1H\}$ (100 MHz)[40] 193.2 (t, $^2J_{CP}$ = 8.8 Hz, *C*O *trans* to CO), 190.6 (t, $^2J_{CP}$ = 6.9 Hz, *C*O *trans* to I), 139.0 (s, *C*H═), 114.6 (s, ═CH_2), 34.0 (s, CH_2), 31.1 (virtual t,[21] $^3J_{CP}$ = 6.1 Hz, $PCH_2CH_2CH_2$), 29.1 (s, CH_2), 29.0 (virtual t,[21] $^1J_{CP}$ = 14.6 Hz, PCH_2)[45], 29.0 (s, CH_2)[45], 24.2 (s, PCH_2CH_2); $^{31}P\{^1H\}$ (121 MHz): −20.9 (s). **IR**: Table 1. **MS**:[39] 1126[41] ([**10a**]$^+$, 20%), 1098[41] ([**10a** − CO]$^+$, 100%), 1000 ([**10a** − I]$^+$, 90%).

*mer,trans-Re(CO)$_3$(I)(P((CH$_2$)$_{14}$)$_3$P) (**11a**). **A**.* A Schlenk flask was charged with **8a** (0.075 g, 0.075 mmol), THF (20 mL), acetone (10 mL), and NaI (0.150 g, 1.00 mmol). The yellow solution was refluxed for 7 d. The solvent was removed from the orange-brown mixture by rotary evaporation and oil pump vacuum. The residue was filtered through Al_2O_3, which was rinsed with THF. The solvent was removed from the combined filtrates by rotary evaporation and oil pump vacuum to give **11a** (0.044 g, 0.042 mmol, 56%) as a pale yellow powder. **B**. A Schlenk flask was charged with **7a** (0.107 g, 0.112 mmol), THF (10 mL), acetone (5 mL), and NaI (0.094 g, 0.63 mmol). The yellow solution was refluxed for 25 h. The solvent was removed from the orange mixture by rotary evaporation and oil pump vacuum. The residue was chromatographed (Al_2O_3 column, 3 × 20 cm, 4:1 v/v hexanes/CH_2Cl_2). The solvent was removed from the product containing fractions by rotary evaporation and oil pump vacuum to give **11a** (0.040 g, 0.038 mmol, 34%) as a pale yellow powder, mp 225 °C, dec (gradual darkening, >173 °C). **TGA**: Table s1. Anal. Calcd (%) for $C_{45}H_{84}IO_3P_2Re$: C 51.56, H 8.08; found C 51.08, H 8.27.

NMR (δ/ppm): ^1H (C_6D_6, 300 MHz)[40] 2.07−1.89 (br m, 12H, PCH_2), 1.80−1.62 (br m, 12H, PCH_2CH_2), 1.60−1.41 (br m, 60H, CH_2). $^{13}C\{^1H\}$ (C_6D_6, 100 MHz)[40] 193.3 (t, $^2J_{CP}$ = 9.3 Hz, *C*O *trans* to CO), 190.3 (t, $^2J_{CP}$ = 6.9 Hz, *C*O *trans* to I), 31.4 (virtual t,[21] $^1J_{CP}$ = 14.7 Hz, PCH_2), 30.3 (virtual t,[21] $^3J_{CP}$ = 6.5 Hz, $PCH_2CH_2CH_2$), 28.8 (s, CH_2), 28.3 (s, CH_2), 28.1 (s, CH_2), 24.2 (s, PCH_2CH_2); $^{31}P\{^1H\}$ (THF-d_8, 121 MHz) −17.2 (s). **IR**: Table 1. **MS**:[39] 1048 ([**11a**]$^+$, 30%), 1020 ([**11a** − CO]$^+$, 100%), 922 ([**11a** − I]$^+$, 30%).

*mer,trans-Re(CO)$_3$(Ph)(P((CH$_2$)$_{14}$)$_3$P) (**12a**).* A Schlenk flask was charged with **7a** (0.075 g, 0.078 mmol), THF (15 mL), and Ph_2Zn (0.091 g, 0.41 mmol). The solution was refluxed for 2 d and cooled. MeOH (5 mL) was added, and a white precipitate formed. The solvent was removed by oil pump vacuum, and the residue was extracted with benzene. The extract was filtered. The solvent was removed from the filtrate by rotary evaporation and oil pump vacuum to give **12a** (0.068 g, 0.068 mmol, 87%) as an orange solid, mp 200 °C, dec (gradual darkening, >172 °C). Anal: calcd (%) for $C_{51}H_{89}O_3P_2Re$: C 61.35, H 8.98; found C 60.38, H 9.74.[42]

NMR (CD_2Cl_2, δ/ppm): ^1H (400 MHz)[40] 7.80 (d, $^3J_{HH}$ = 6.0 Hz, 2H, *o*-Ph), 6.87−6.83 (m, 3H, *m*-Ph and *p*-Ph), 1.89−1.84 (br m, 4H, PCH_2[49]), 1.61−1.50 (br m, 12H, CH_2), 1.50−1.21 (br m, 68H, CH_2); $^{13}C\{^1H\}$ (100 MHz)[40] 198.2 (t, $^2J_{CP}$ = 9.3 Hz, *C*O *trans* to CO), 196.6 (t, $^2J_{CP}$ = 5.6 Hz, *C*O *trans* to Ph), 157.7 (t, $^2J_{CP}$ = 11.8 Hz, *i*-Ph), 147.0 (s, *o*-Ph), 126.8 (s, *m*-Ph),[50] 121.4 (s, *p*-Ph), 32.6 (virtual t,[21] $^1J_{CP}$ = 14.2 Hz, PCH_2), 30.4 (virtual t,[21] $^3J_{CP}$ = 6.5 Hz, $PCH_2CH_2CH_2$), 30.1 (virtual t,[21] $^3J_{CP}$ = 6.5 Hz, $PCH_2CH_2CH_2$), 29.6 (virtual t,[21] $^1J_{CP}$ = 14.5 Hz, PCH_2), 29.1 (s, CH_2), 28.9 (s, CH_2), 28.57 (s, CH_2), 28.56 (s, CH_2), 28.21 (s, CH_2), 28.20 (s, CH_2), 28.15 (s, CH_2), 28.0 (s, CH_2), 24.0 (s, PCH_2CH_2), 22.7 (s, PCH_2CH_2); $^{31}P\{^1H\}$ (121 MHz): −12.3 (s). **IR**: Table 1. **MS**:[39] 999 ([**12a**]$^+$, 50%), 971 ([**12a** − CO]$^+$, 40%), 943 ([**12a** − 2CO]$^+$, 25%), 922 ([**12a** − Ph]$^+$, 40%), 684 ([P((CH$_2$)$_{16}$)P + 2O]$^+$, 100%).

*mer,trans-Re(CO)$_3$(Me)(P((CH$_2$)$_{14}$)$_3$P) (**13a**). **A**.* A Schlenk flask was charged with **8a** (0.100 g, 0.100 mmol), THF (10 mL), and MeLi (1.6 M in Et_2O; 0.625 mL, 0.022 g, 1.00 mmol). The white emulsion was stirred for 2 d. Water was carefully added to hydrolyze the excess MeLi. The organic layer was filtered through Al_2O_3 and $MgSO_4$. The solvent was removed from the filtrate by oil pump vacuum to give **13a** (0.077 g, 0.082 mmol, 82%) as a white powder. **B**. A Schlenk flask was charged with **7a** (0.099 g, 0.10 mmol), THF (10 mL), and MeLi (1.6 M in Et_2O; 0.625 mL, 0.022 g, 1.00 mmol). The white emulsion was stirred for 24 h. Workup as in procedure **A** gave **13a** (0.075 g, 0.080 mmol, 78%) as a white powder, mp 175 °C, dec (gradual darkening, >149 °C). **DSC/TGA**: Table s1. Anal. Calcd (%) for $C_{46}H_{87}O_3P_2Re$: C 59.01, H 9.37; found C 58.61, H 9.38.

NMR (C_6D_6, δ/ppm): ^1H (300 MHz)[40] 1.82−1.68 (br m, 12H, PCH_2), 1.67−1.55 (br m, 12H, PCH_2CH_2), 1.53−1.31 (br m, 60H, CH_2), −0.27 (t, $^3J_{HP}$ = 6.0 Hz, $ReCH_3$); $^{13}C\{^1H\}$ (100 MHz)[40] 201.1 (t, $^2J_{CP}$ = 9.2 Hz, *C*O *trans* to CO), 195.8 (t, $^2J_{CP}$ = 7.5 Hz, *C*O *trans* to Me), 30.9−30.3[51] (m, $PCH_2/PCH_2CH_2CH_2$), 28.6 (s, CH_2), 28.4 (s, CH_2), 28.1 (s, CH_2), 27.9 (s, CH_2), 23.9 (s, PCH_2CH_2), −31.9 (t, $^2J_{CP}$ = 6.4 Hz, $ReCH_3$); $^{31}P\{^1H\}$ (121 MHz): −8.7 (s). **IR**: Table 1. **MS**:[39] 936[41] ([**13a**]$^+$, 4%), 921[41] ([**13a** − Me]$^+$, 40%), 908[41] ([**13a** − CO]$^+$, 8%), 683[41] ([P((CH$_2$)$_{16}$)P + 2O]$^+$, 100%), 667[41] ([P((CH$_2$)$_{16}$)P + O]$^+$, 45%), 651[41] ([P((CH$_2$)$_{16}$)P]$^+$, 10%).

Crystallography. A. A hexanes/CH_2Cl_2 solution of **7a** was heated to 40 °C and concentrated under reduced pressure (560 mbar) with cooling. After 30 min, colorless prisms were collected. Data were acquired as outlined in Table s2. Cell parameters were obtained from 10 frames using a 10° scan and refined with 9685 reflections. Lorentz, polarization, and absorption corrections[52] were applied. The space group was determined from systematic absences and subsequent least-squares refinement. The structure was solved by direct methods. The parameters were refined with all data by full-matrix-least-squares on F^2 using SHELXL-97.[53] Non-hydrogen atoms were refined with anisotropic thermal parameters. The hydrogen atoms were fixed in idealized positions using a riding model. Some strong residual electron densities were apparent, but were presumed to be artifacts. Scattering factors were taken from the literature.[54] **B**. A CH_2Cl_2 solution of **8a** was layered with MeOH. After two weeks, colorless prisms were collected. Data were acquired, and the structure was solved, as in **A** (10 frames, 10° scan, 9139 reflections). The bromide ligand was disordered over three positions, and refinement indicated a 70:15:15 occupancy. The carbonyl ligands were located and assigned corresponding occupancies (30:85:85). **C**. A THF solution of **12a** was layered with MeOH. After 1 d, colorless prisms were collected. Data were acquired, and the structure was solved, as in **A** (10 frames, 10° scan, 25525 reflections). Four independent molecules of **12a** and four independent molecules of THF were present in the asymmetric unit (two asymmetric units/unit cell). The chiral space group was refined as a racemic twin (Flack's absolute structure parameter: 0.412).[55] **D**. A CH_2Cl_2 solution of **13a** was layered with MeOH. After two weeks, colorless prisms were collected. Data were acquired, and the structure was solved, as in **A** (10 frames, 10° scan, 9646 reflections). The methyl group and one carbonyl ligand were disordered over two positions (see text) and refined to a 55:45 occupancy ratio.

■ ASSOCIATED CONTENT

Supporting Information

The Supporting Information is available free of charge on the ACS Publications website at DOI: 10.1021/acs.inorgchem.7b00909.

Experimental procedures, representative IR and NMR spectra and tables of thermal properties and characterization and crystallographic data (PDF)

Accession Codes

CCDC 669204−669206 and 1541799 contain the supplementary crystallographic data for this paper. These data can be obtained free of charge via www.ccdc.cam.ac.uk/data_request/cif, or by emailing data_request@ccdc.cam.ac.uk, or by contacting The Cambridge Crystallographic Data Centre, 12 Union Road, Cambridge CB2 1EZ, UK; fax: +44 1223 336033.

■ AUTHOR INFORMATION

Corresponding Author

*E-mail: gladysz@mail.chem.tamu.edu.

ORCID

Tobias Fiedler: 0000-0001-7169-305X

John A. Gladysz: 0000-0002-7012-4872

DOI: 10.1021/acs.inorgchem.7b00909
Inorg. Chem. 2017, 56, 7454−7469

Notes

The authors declare no competing financial interest.

■ ACKNOWLEDGMENTS

The authors thank the U.S. National Science Foundation (CHE-0719267, CHE-1153085, CHE-156601) and Deutsche Forschungsgemeinschaft (DFG, GL 300/9-1) for support.

■ REFERENCES

(1) Kottas, G. S.; Clarke, L. I.; Horinek, D.; Michl, J. Artificial Molecular Rotors. *Chem. Rev.* **2005**, *105*, 1281−1376.

(2) (a) de Jonge, J. J.; Ratner, M. A.; de Leeuw, S. W. Local Field Controlled Switching in a One-Dimensional Dipolar Array. *J. Phys. Chem. C* **2007**, *111*, 3770−3777. (b) Khan, N. S.; Perez-Aguilar, J. M.; Kaufmann, T.; Hill, P. A.; Taratula, O.; Lee, O.-S.; Carroll, P. J.; Saven, J. G.; Dmochowski, I. J. Multiple Hindered Rotators in a Gyroscope-Inspired Tribenzylamine Hemicryptophane. *J. Org. Chem.* **2011**, *76*, 1418−1424. (c) Dial, B. E.; Pellechia, P. J.; Smith, M. D.; Shimizu, K. D. Proton Grease: An Acid Accelerated Molecular Rotor. *J. Am. Chem. Soc.* **2012**, *134*, 3675−3678. (d) Zhang, Q.-C.; Wu, F.-T.; Hao, H.-M.; Xu, H.; Zhao, H.-X.; Long, L.-S.; Huang, R.-B.; Zheng, L. S. Modulating the Rotation of a Molecular Rotor through Hydrogen-Bonding Interactions between the Rotator and Stator. *Angew. Chem., Int. Ed.* **2013**, *52*, 12602−12605. (e) Chen, F.; García-López, V.; Jin, T.; Neupane, B.; Chu, P.-L. E.; Tour, J.; Wang, G. Moving Kinetics of Nanocars with Hydrophobic Wheels on Solid Surfaces at Ambient Conditions. *J. Phys. Chem. C* **2016**, *120*, 10887−10894. (f) Meshkov, I. N.; Bulach, V.; Gorbunova, Y. G.; Kyritsakas, N.; Grigoriev, M. S.; Tsivadze, A. Y.; Hosseini, M. W. Phosphorus(V) Porphyrin-Based Molecular Turnstiles. *Inorg. Chem.* **2016**, *55*, 10774−10782. (g) Wang, G.; Xiao, H.; He, J.; Xiang, J.; Wang, Y.; Chen, X.; Che, Y.; Jiang, H. Molecular Turnstiles Regulated by Metal Ions. *J. Org. Chem.* **2016**, *81*, 3364−3371.

(3) A cross section of recent applications from an extensive literature: (a) Lee, S.-C.; Heo, J.; Ryu, J.-W.; Lee, C.-L.; Kim, S.; Tae, J.-S.; Rhee, B.-O.; Kim, S.-W.; Kwon, O.-P. Pyrrolic molecular rotors acting as viscosity sensors with high fluorescence contrast. *Chem. Commun.* **2016**, *52*, 13695−13698. (b) Kim, T.-I.; Maity, S. B.; Bouffard, J.; Kim, Y. Molecular Rotors for the Detection of Chemical Warfare Agent Simulants. *Anal. Chem.* **2016**, *88*, 9259−9263. (c) Qian, H.; Cousins, M. E.; Horak, E. H.; Wakefield, A.; Liptak, M. D.; Aprahamian, I. Suppression of Kasha's rule as a mechanism for fluorescent molecular rotors and aggregation-induced emission. *Nat. Chem.* **2016**, *9*, 83−87. (d) Ibarra-Rodriguez, M.; Muñoz-Flores, B.; Dias, H. V. R.; Sánchez, M.; Gomez-Treviño, A.; Santillan, R.; Farfán, N.; Jiménez-Pérez, V. M. Fluorescent Molecular Rotors of Organoboron Compounds from Schiff Bases: Synthesis, Viscosity, Reversible Thermochromism, Cytotoxicity, and Bioimaging Cells. *J. Org. Chem.* **2017**, *82*, 2375−2385.

(4) Recent lead references: (a) Kistemaker, J. C. M.; Štacko, P.; Visser, J.; Feringa, B. L. Unidirectional rotary motion in achiral molecular motors. *Nat. Chem.* **2015**, *7*, 890−896. (b) Faulkner, A.; van Leeuwen, T.; Feringa, B. L.; Wezenberg, S. J. Allosteric Regulation of the Rotational Speed in a Light-Driven Molecular Motor. *J. Am. Chem. Soc.* **2016**, *138*, 13597−13603. (c) Collins, B. S. L.; Kistemaker, J. C. M.; Otten, E.; Feringa, B. L. A chemically powered unidirectional rotary molecular motor based on a palladium redox cycle. *Nat. Chem.* **2016**, *8*, 860−866.

(5) (a) Khuong, T.-A. V.; Nuñez, J. E.; Godinez, C. E.; Garcia-Garibay, M. A. Crystalline Molecular Machines: A Quest Toward Solid-State Dynamics and Function. *Acc. Chem. Res.* **2006**, *39*, 413−422. (b) Nuñez, J. E.; Natarajan, A.; Khan, S. I.; Garcia-Garibay, M. A. Synthesis of a Triply-Bridged Molecular Gyroscope by a Directed Meridional Cyclization Strategy. *Org. Lett.* **2007**, *9*, 3559−3561. (c) Vogelsberg, C. S.; Garcia-Garibay, M. A. Crystalline molecular machines: function, phase order, dimensionality, and composition. *Chem. Soc. Rev.* **2012**, *41*, 1892−1910. (d) Pérez-Estrada, S.; Rodríguez-Molina, B.; Xiao, L.; Santillan, R.; Jiménez-Osés, G.; Houk, K. N.; Garcia-Garibay, M. A. Thermodynamic Evaluation of Aromatic CH/π Interactions and Rotational Entropy in a Molecular Rotor. *J. Am. Chem. Soc.* **2015**, *137*, 2175−2178. (e) Arcos-Ramos, R.; Rodríguez-Molina, B.; Gonzalez-Rodriguez, E.; Ramirez-Montes, P. I.; Ochoa, M. E.; Santillan, R.; Farfán, N.; Garcia-Garibay, M. A. Crystalline arrays of molecular rotors with TIPS-trityl and phenolic-trityl stators using phenylene, 1,2-difluorophenylene and pyridine rotators. *RSC Adv.* **2015**, *5*, 55201−55208. (f) Jiang, X.; O'Brien, Z. J.; Yang, S.; Lai, L. H.; Buenaflor, J.; Tan, C.; Khan, S.; Houk, K. N.; Garcia-Garibay, M. A. Crystal Fluidity Reflected by Fast Rotational Motion at the Core, Branches, and Peripheral Aromatic Groups of a Dendrimeric Molecular Rotor. *J. Am. Chem. Soc.* **2016**, *138*, 4650−4656. (g) Catalano, L.; Perez-Estrada, S.; Wang, H.-H.; Ayitou, A. J.-L.; Khan, S. I.; Terraneo, G.; Metrangolo, P.; Brown, S.; Garcia-Garibay, M. A. Rotational Dynamics of Diazabicyclo[2.2.2]-octane in Isomorphous Halogen-Bonded Co-crystals: Entropic and Enthalpic Effects. *J. Am. Chem. Soc.* **2017**, *139*, 843−848.

(6) (a) Setaka, W.; Yamaguchi, K. Order−Disorder Transition of Dipolar Rotor in a Crystalline Molecular Gyrotop and Its Optical Change. *J. Am. Chem. Soc.* **2013**, *135*, 14560−14563. and earlier work cited therein. (b) Setaka, W.; Inoue, K.; Higa, S.; Yoshigai, S.; Kono, H.; Yamaguchi, K. Synthesis of Crystalline Molecular Gyrotops and Phenylene Rotation inside the Cage. *J. Org. Chem.* **2014**, *79*, 8288−8295. (c) Setaka, W.; Higa, S.; Yamaguchi, K. Ring-closing metathesis for the synthesis of a molecular gyrotop. *Org. Biomol. Chem.* **2014**, *12*, 3354−3357. (d) Shionari, H.; Inagaki, Y.; Yamaguchi, K.; Setaka, W. A pyrene-bridged macrocage showing no excimer fluorescence. *Org. Biomol. Chem.* **2015**, *13*, 10511−10516. (e) Nishiyama, Y.; Inagaki, Y.; Yamaguchi, K.; Setaka, W. 1,4-Naphthalenediyl-Bridged Molecular Gyrotops: Rotation of the Rotor and Fluorescence in Solution. *J. Org. Chem.* **2015**, *80*, 9959−9966. (f) Masuda, T.; Arase, J.; Inagaki, Y.; Kawahata, M.; Yamaguchi, K.; Ohhara, T.; Nakao, A.; Momma, H.; Kwon, E.; Setaka, W. Molecular Gyrotops with a Five-Membered Heteroaromatic Ring: Synthesis, Temperature-Dependent Orientation of Dipolar Rotors inside the Crystal, and its Birefringence Change. *Cryst. Growth Des.* **2016**, *16*, 4392−4401.

(7) Prack, E.; O'Keefe, C. A.; Moore, J. K.; Lai, A.; Lough, A. J.; Macdonald, P. M.; Conradi, M. S.; Schurko, R. W.; Fekl, U. A Molecular Rotor Possessing an H−M−H "Spoke" on a P−M−P "Axle": A Platinum(II) *trans*-Dihydride Spins Rapidly Even at 75 K. *J. Am. Chem. Soc.* **2015**, *137*, 13464−13467.

(8) (a) Shima, T.; Hampel, F.; Gladysz, J. A. Molecular Gyroscopes: $Fe(CO)_3$ and $Fe(CO)_2(NO)^+$ Rotators Encased in Three-Spoke Stators; Facile Assembly via Alkene Metatheses. *Angew. Chem., Int. Ed.* **2004**, *43*, 5537−5540. (b) Lang, G. M.; Shima, T.; Wang, L.; Cluff, K. J.; Hampel, F.; Blümel, J.; Gladysz, J. A. Gyroscope Like Complexes based upon Dibridgehead Diphosphine Cages that are Accessed by Three Fold Intramolecular Ring Closing Metatheses and Encase $Fe(CO)_3$, $Fe(CO)_2(NO)^+$ and $Fe(CO)_3(H)^+$ Rotators. *J. Am. Chem. Soc.* **2016**, *138*, 7649−7663. (c) Lang, G. M.; Skaper, D.; Hampel, F.; Gladysz, J. A. Synthesis, Reactivity, Structures, and Dynamic Properties of Gyroscope Like Iron Complexes with Dibridgehead Diphosphine Cages: Pre- vs. Post-Metathesis Substitutions as Routes to Adducts with Neutral Dipolar Fe(CO)(NO)(X) Rotors. *Dalton Trans.* **2016**, *45*, 16190−16204.

(9) (a) Nawara, A. J.; Shima, T.; Hampel, F.; Gladysz, J. A. Gyroscope-Like Molecules Consisting of PdX_2/PtX_2 Rotators Encased in Three-Spoke Stators: Synthesis via Alkene Metathesis, and Facile Substitution and Demetalation. *J. Am. Chem. Soc.* **2006**, *128*, 4962−4963. (b) Stollenz, M.; Barbasiewicz, M.; Nawara-Hultzsch, A. J.; Fiedler, T.; Laddusaw, R. M.; Bhuvanesh, N.; Gladysz, J. A. Dibridgehead Diphosphines that Turn Themselves Inside-Out. *Angew. Chem., Int. Ed.* **2011**, *50*, 6647−6651. (c) Nawara-Hultzsch, A. J.; Stollenz, M.; Barbasiewicz, M.; Szafert, S.; Lis, T.; Hampel, F.; Bhuvanesh, N.; Gladysz, J. A. Gyroscope Like Molecules Consisting of PdX_2/PtX_2 Rotators Within Three-Spoke Dibridgehead Diphosphine Stators: Syntheses, Substitution Reactions, Structures, and Dynamic Properties. *Chem. - Eur. J.* **2014**, *20*, 4617−4637. (d) Taher, D.; Nawara-Hultzsch, A. J.; Bhuvanesh, N.; Hampel, F.; Gladysz, J. A. Mono- and Disubstitution Reactions of Gyroscope Like Complexes Derived from Cl-Pt-Cl Rotators within Cage Like Dibridgehead Diphosphine Ligands. *J. Organomet. Chem.* **2016**, *821*, 136−141. (e) Kharel, S.; Joshi, H.;

DOI: 10.1021/acs.inorgchem.7b00909
Inorg. Chem. 2017, 56, 7454−7469

Bierschenk, S.; Stollenz, M.; Taher, D.; Bhuvanesh, N.; Gladysz, J. A. Homeomorphic Isomerization as a Design Element in Container Molecules; Binding, Displacement, and Selective Transport of MCl_2 Species (M = Pt, Pd, Ni). *J. Am. Chem. Soc.* **2017**, *139*, 2172−2175.
(10) Wang, L.; Hampel, F.; Gladysz, J. A. "Giant" Gyroscope-Like Molecules Consisting of Dipolar Cl-Rh-CO Rotators Encased in Three-Spoke Stators That Define 25−27 Membered Macrocycles. *Angew. Chem., Int. Ed.* **2006**, *45*, 4372−4375.
(11) (a) Wang, L.; Shima, T.; Hampel, F.; Gladysz, J. A. Gyroscope-Like Molecules Consisting of Three-Spoke Stators that Enclose "Switchable" Neutral Dipolar Rhodium Rotators; Reversible Cycling between Faster and Slower Rotating Rh(CO)I and $Rh(CO)_2I$ Species. *Chem. Commun.* **2006**, 4075−4077. (b) Estrada, A. L.; Jia, T.; Bhuvanesh, N.; Blümel, J.; Gladysz, J. A. Substitution and Catalytic Chemistry of Gyroscope Like Complexes Derived from Cl-Rh-CO Rotators and Triply *trans* Spanning Di(trialkylphosphine) Ligands. *Eur. J. Inorg. Chem.* **2015**, *2015*, 5318−5321.
(12) Hess, G. D.; Hampel, F.; Gladysz, J. A. Octahedral Gyroscope-Like Molecules with $M(CO)_3(X)$ Rotators Encased in Three-Spoked Diphosphine Stators: Syntheses by Alkene Metathesis/Hydrogenation Sequences, Structures, Dynamic Properties, and Reactivities. *Organometallics* **2007**, *26*, 5129−5131.
(13) (a) Fiedler, T.; Bhuvanesh, N.; Hampel, F.; Reibenspies, J. H.; Gladysz, J. A. Gyroscope Like Molecules Consisting of Trigonal or Square Planar Osmium Rotators Within Three-Spoked Dibridgehead Diphosphine Stators: Syntheses, Substitution Reactions, Structures, and Dynamic Properties. *Dalton Trans.* **2016**, *45*, 7131−7147. (b) Fiedler, T.; Chen, L.; Wagner, N. D.; Russell, D. R.; Gladysz, J. A. Gas and Liquid Phase Diffusivities of Isomeric Metal Complexes Derived from Multifold Ring Closing Metatheses: Ion Mobility Mass Spectrometry Trumps DOSY NMR. *Organometallics* **2016**, *35*, 2071−2075.
(14) See also (a) Lang, G. M.; Bhuvanesh, N.; Reibenspies, J. H.; Gladysz, J. A. Syntheses, Reactivity, Structures, and Dynamic Properties of Gyroscope Like Iron Carbonyl Complexes based upon Dibridgehead Diarsine Cages. *Organometallics* **2016**, *35*, 2873−2889. (b) Zeits, P. D.; Rachiero, G. P.; Hampel, F.; Reibenspies, J. H.; Gladysz, J. A. Gyroscope-Like Platinum and Palladium Complexes with *trans*-Spanning Bis(Pyridine) Ligands. *Organometallics* **2012**, *31*, 2854−2877.
(15) Schmidt, S. P.; Trogler, W. C.; Basolo, F. Pentacarbonylrhenium halides. *Inorg. Synth.* **1985**, *23*, 41−46.
(16) (a) Reimann, R. H.; Singleton, E. Transition metal carbonyls IV. Substitution reactions of rhenium pentacarbonyl bromide. *J. Organomet. Chem.* **1973**, *59*, 309−315. (b) Yamazaki, Y.; Morimoto, T.; Ishitani, O. Synthesis of novel photofunctional multinuclear complexes using a coupling reaction. *Dalton Trans.* **2015**, *44*, 11626−11635.
(17) Nawara-Hultzsch, A. J.; Skopek, K.; Shima, T.; Barbasiewicz, M.; Hess, G. D.; Skaper, D.; Gladysz, J. A. Syntheses and Palladium, Platinum, and Borane Adducts of Symmetrical Trialkylphosphines with Three Terminal Vinyl Groups, $P((CH_2)_mCH{=}CH_2)_3$. *Z. Naturforsch., B: J. Chem. Sci.* **2010**, *65*, 414−424.
(18) Adams, D. M. *Metal-Ligand and Related Vibrations;* St. Martin's Press: New York, 1968; Chapter 3.
(19) Bond, A. M.; Colton, R.; McDonald, M. E. Chemical and Electrochemical Studies of Tricarbonyl Derivatives of Manganese and Rhenium. *Inorg. Chem.* **1978**, *17*, 2842−2847.
(20) When the reactions of $Re(CO)_5(X)$ and **1a** are conducted under milder conditions (chlorobenzene, 60−80 °C), *fac*-**2a** and *fac*-**3a** are isolated (43−67%). See Chapter 3 of ref 27. For similar examples of *fac*/*mer* selectivity, see ref 16a.
(21) The *J* values given for the virtual triplets represent the *apparent* couplings between adjacent peaks and not the mathematically rigorous coupling constants. Hersh, W. H. False AA'X Spin−Spin Coupling Systems in ^{13}C NMR: Examples Involving Phosphorus and a 20-Year-Old Mystery in Off-Resonance Decoupling. *J. Chem. Educ.* **1997**, *74*, 1485−1488.
(22) (a) Hund, H.-U.; Ruppli, U.; Berke, H. Chemistry of (Carbonyl)(nitrosyl)[bis(phosphorus donor)]rhenium Complexes. *Helv. Chim. Acta* **1993**, *76*, 963−975. (b) Southern, J. S.; Green, M. T.; Hillhouse, G. L.; Guzei, I. A.; Rheingold, A. L. Chemistry of Coordinated Nitroxyl. Reagent-Specific Protonations of *trans*-$Re(CO)_2(NO)(PR_3)_2$ (R = Ph, Cy) That Give the Neutral Nitroxyl Complexes *cis,trans*-$ReCl(CO)_2(NH{=}O)(PR_3)_2$ or the Cationic Hydride Complex [*trans,trans*-$ReH(CO)_2(NO)(PPh_3)_2^+][SO_3CF_3^-]$. *Inorg. Chem.* **2001**, *40*, 6039−6046.
(23) The first stereochemical descriptor (*cis*) refers to the relationship of the chloride ligands, and the second (*trans*) refers to the phosphine ligands.
(24) DSC and TGA data have been treated as recommended by Cammenga, H. K.; Epple, M. Basic Principles of Thermoanalytical Techniques and Their Applications in Preparative Chemistry. *Angew. Chem., Int. Ed. Engl.* **1995**, *34*, 1171−1187.
(25) (a) Huhmann-Vincent, J.; Scott, B. L.; Kubas, G. J. Rhenium Complexes with Weakly Coordinating Solvent Ligands, *cis*-$[Re(PR_3)(CO)_4(L)][BAr_F]$, L = CH_2Cl_2, Et_2O, NC_5F_5: Decomposition to Chloride-Bridged Dimers in CH_2Cl_2 Solution. *Inorg. Chem.* **1999**, *38*, 115−124. (b) Choualeb, A.; Blacque, O.; Schmalle, H. W.; Fox, T.; Hiltebrand, T.; Berke, H. Olefin Complexes of Low-Valent Rhenium. *Eur. J. Inorg. Chem.* **2007**, *2007*, 5246−5261.
(26) (a) Parker, D. W.; Marsi, M. M.; Gladysz, J. A. Substitution Mechanisms at Metal Carbonyl Centers; Conversion of $Ph_3P(CO)_4ReBr$ to $Ph_3P(CO)_4ReCH_3$ via an Anionic Acyl Intermediate. *J. Organomet. Chem.* **1980**, *194*, C1−4. (b) Ramsden, J. A.; Peng, T.-S.; Gladysz, J. A. Reactions of Rhenium Halide Complexes $(\eta^5\text{-}C_5H_5)Re(NO)(PPh_3)(X)$ and Organocopper Nucleophiles; New Routes to Racemic and Optically Active Hydrocarbyl Complexes $(\eta^5\text{-}C_5H_5)Re(NO)(PPh_3)(R)$. *Bull. Soc. Chim. Fr.* **1992**, *129*, 625−631. (c) Ruwwe, J.; Martín-Alvarez, J. M.; Horn, C. R.; Bauer, E.; Szafert, S.; Lis, T.; Hampel, F.; Cagle, P. C.; Gladysz, J. A. Olefin Metatheses in Metal Coordination Spheres: Versatile New Strategies for the Construction of Novel Monohapto or Polyhapto Cyclic, Macrocyclic, Polymacrocyclic, and Bridging Ligands. *Chem. - Eur. J.* **2001**, *7*, 3931−3950.
(27) Heß, G. D. U. Syntheses of Rhenium Containing Gyroscope-like Complexes, and Related Species. Doctoral Dissertation, Universität Erlangen-Nürnberg: Erlangen, Germany, 2010.
(28) (a) Mink, R. I.; Welter, J. J.; Young, P. R.; Stucky, G. D. Metalation of Bis(cyclopentadienyl)metal Hydrides by *n*-Butyllithium in the Presence of Pentamethyldiethylenetriamine. Synthesis of Bis(cyclopentadienyl)rhenium Alkyls and the Mixed Metal Complexes: $(\eta^5\text{-}C_5H_5)_2M(\mu\text{-}CO)_2Re(CO)(\eta^5\text{-}C_5H_5)$ (M = Mo, W). *J. Am. Chem. Soc.* **1979**, *101*, 6928−6933. (b) Meyer, W. E.; Amoroso, A. J.; Jaeger, M.; Le Bras, J.; Wong, W.-T.; Gladysz, J. A. Synthesis and Oxidation of Chiral Rhenium Phosphine Methyl Complexes of the Formula $(\eta^5\text{-}C_5Me_5)Re(NO)(PR_3)(CH_3)$: In Search of Radical Cations with Enhanced Kinetic Stabilities. *J. Organomet. Chem.* **2000**, *616*, 44−53.
(29) (a) Dunitz, J. D.; Maverick, E. F.; Trueblood, K. N. Atomic Motions in Molecular Crystals from Diffraction Measurements. *Angew. Chem., Int. Ed. Engl.* **1988**, *27*, 880−895. (b) Ananchenko, G. S.; Udachin, K. A.; Pojarova, M.; Jebors, S.; Coleman, A. W.; Ripmeester, J. A. A molecular turnstile in *para*-octanoyl calix[4]arene nanocapsules. *Chem. Commun.* **2007**, 707−709.
(30) The specific complexes were *mer,trans*-$Re(CO)_3(Cl)(P((CH_2)_4CH{=}CH_2)_3)_2$, *mer,trans*-$Re(CO)_3(Cl)(P((CH_2)_5CH{=}CH_2)_3)_2$, and *mer,trans*-$Re(CO)_3(Br)(P((CH_2)_5CH{=}CH_2)_3)_2$. The last two were pure by $^{31}P\{^1H\}$ NMR, and the first was ca. 83% pure.[27]
(31) (a) Jung, J. H.; Ono, Y.; Shinkai, S. Influence of an Odd-Even Relationship on the Aggregation Modes of "Gemini"-type Cholestrol-Based Gelators and Their Transcription into Silica Gel. *Chem. Lett.* **2000**, *29*, 636−637. (b) Aoki, K.; Kudo, M.; Tamaoki, N. Novel Odd/Even Effect of Alkylene Chain Length on the Photopolymerizability of Organogelators. *Org. Lett.* **2004**, *6*, 4009−4012. (c) Thalladi, V. R.; Nüsse, M.; Boese, R. The Melting Point Alternation in α,ω-Alkanedicarboxylic Acids. *J. Am. Chem. Soc.* **2000**, *122*, 9227−9236.
(32) Some of the C-O distances in Table 2 are clearly affected by disorder. For this and other reasons, average ReCO distances are employed in calculating the radius of the rotator, as opposed to the longest distance as often used in earlier papers.
(33) Bondi, A. van der Waals Volumes and Radii. *J. Phys. Chem.* **1964**, *68*, 441−451.

DOI: 10.1021/acs.inorgchem.7b00909
Inorg. Chem. 2017, 56, 7454−7469

(34) Some readers will note the inclusion of the *para* hydrogen atom in estimating the radius of the phenyl substituted rotator, but not any of the methyl hydrogen atoms for the methyl substituted rotator. With methyl ligands, the hydrogen atoms do not add much additional volume in a horizontal direction; the CO ligands are more extended in any case. With phenyl ligands, the *para* hydrogen atom does significantly extend the volume in a horizontal direction.
(35) It might be argued that subtracting the van der Waals radius of carbon from the average of the six values might give a better reflection of the interior space available in solution. On the other hand, the smallest value gives the most conservative estimate of the void space.
(36) (a) Ansyln, E. V.; Dougherty, D. A. *Modern Physical Organic Chemistry*; University Science Books: Sausalito, CA, 2006; pp 97−98. (b) Eliel, E. N.; Wilen, S. H. *Stereochemistry of Organic Compounds*; Wiley: New York, 1994; pp 624−629 and 1142−1155. (c) All twelve rotational minima of a complex with the same symmetry as **9a**, **10a**, and **14a**, are depicted in Figure 19 of reference 14a.
(37) (a) Kanu, A. B.; Dwivedi, B.; Tam, M.; Matz, L.; Hill, H. H., Jr. Ion mobility−mass spectrometry. *J. Mass Spectrom.* **2008**, *43*, 1−22. (b) Lanucara, F.; Holman, S. W.; Gray, C. J.; Eyers, C. E. The power of ion mobility-mass spectrometry for structural characterization and the study of conformational dynamics. *Nat. Chem.* **2014**, *6*, 281−294.
(38) The ^{1}H and ^{13}C{^{1}H} NMR assignments were made by ^{1}H,^{1}H COSY and ^{1}H,^{13}C {^{1}H} COSY experiments.
(39) FAB, 3-NBA, *m*/*z* (relative intensity, %); the most intense peak of the isotope envelope is given.
(40) The ^{1}H and ^{13}C{^{1}H} NMR assignments were made by analogy to those of **2a** or **7a**,
(41) The most intense peak of some ions differs by 1−2 mass units from that calculated for the assigned composition. This is ascribed to instrumental issues and/or the presence of + H ions, as detailed in reference 27.
(42) These three microanalyses poorly agree with the empirical formula, but are nonetheless reported as the best obtained to date. The NMR spectra indicate high purities (≥ 98%), as exemplified in the Supporting Information for **12a**. See also. Gabbaï, F. P.; Chirik, P. J.; Fogg, D. E.; Meyer, K.; Mindiola, D. J.; Schafer, L. L.; You, S.-L. An Editorial About Elemental Analysis. *Organometallics* **2016**, *35*, 3255−3256.
(43) MALDI, *m*/*z* (relative intensity, %); the most intense peak of the isotope envelope is given.
(44) Crude mixture of isomers as depicted in Scheme 1.
(45) These signals overlap, such that the outer peaks of the triplet are visible on each side of a broadened central peak.
(46) The reaction was performed with a balloon pressure of H_2 (1 bar) as opposed to Fischer−Porter bottle and H_2 (5 bar).
(47) A ^{31}P{^{1}H} NMR signal with a plausible chemical shift for **7b** was detected in the crude mixture (ca. 20% of the total integration); see Figure s6.
(48) One peak of this triplet is obscured, and the chemical shift and coupling constant are extrapolated from the two that are visible.
(49) As noted in the text, one methylene chain of this complex gives a set of NMR signals distinct from the other two. The remaining PCH_2 signals overlap with CH_2 signals more remote from phosphorus.
(50) The ^{13}C NMR signal with the chemical shift closest to benzene is assigned to the *meta* carbon. See Mann, B. E. The Carbon-13 and Phosphorus-31 Nuclear Magnetic Resonance Spectra of Some Tertiary Phosphines. *J. Chem. Soc., Perkin Trans. 2* **1972**, 30−34.
(51) These two virtual triplets overlap, such that the apparent *J* values could not be determined.
(52) (a) Hooft, R. W. W. *Collect*; data collection software; Nonius BV: Delft, Netherlands, 1998. (b) Otwinowski, Z.; Minor, W. In *Methods in Enzymology*; Carter, C. W., Jr.; Sweet, R. M., Eds.; Macromolecular Crystallography, Vol. *276*, Part A; Academic Press: New York, 1997; pp 307−326.
(53) Sheldrick, G. M. Crystal structure refinement with SHELXL. *Acta Crystallogr., Sect. C: Struct. Chem.* **2015**, *C71*, 3−8.
(54) Cromer, D. T.; Waber, J. T. In *International Tables for X-ray Crystallography*; Ibers, J. A., Hamilton, W. C., Eds.; Kynoch: Birmingham, England, 1974.
(55) Flack, H. D. On Enantiomorph-Polarity Estimation. *Acta Crystallogr., Sect. A: Found. Crystallogr.* **1983**, *A39*, 876−881.

DOI: 10.1021/acs.inorgchem.7b00909
Inorg. Chem. 2017, 56, 7454−7469